NASA TECHNICAL NOTE

NASA TN D-2759

NASA TN D-2759

DETERMINATION OF THE ELLIPTICITY OF THE EARTH'S EQUATOR FROM OBSERVATIONS ON THE DRIFT OF THE SYNCOM II SATELLITE

by Carl A. Wagner

Goddard Space Flight Center

Greenbelt, Md.

NATIONAL AERONAUTICS AND SPACE ADMINISTRATION • WASHINGTON, D. C. • MAY 1965

NASA TN D-2759

DETERMINATION OF THE ELLIPTICITY OF THE EARTH'S EQUATOR FROM OBSERVATIONS ON THE DRIFT OF THE SYNCOM II SATELLITE

By Carl A. Wagner

Goddard Space Flight Center
Greenbelt, Md.

NATIONAL AERONAUTICS AND SPACE ADMINISTRATION

For sale by the Clearinghouse for Federal Scientific and Technical Information
Springfield, Virginia 22151 – Price $3.00

DETERMINATION OF THE ELLIPTICITY OF THE EARTH'S EQUATOR FROM OBSERVATIONS ON THE DRIFT OF THE SYNCOM II SATELLITE

by
Carl A. Wagner
Goddard Space Flight Center

SUMMARY

23712

An original, simple theory is presented for the radial and longitudinal drift regime, in a triaxial earth-gravity field, of an inclined 24-hour satellite with a near-circular orbit. The drift regime equations for an equatorial satellite (derived by more complex perturbation methods) have been known for at least 2 years. This new theory shows that the "inclined orbit" regime is the same as the equatorial, modified only by an "inclination factor."

The theory is closely validated by two numerically integrated particle drifts of about 3 months duration each, starting with the elements of Syncom II for epochs 26.709 August 1963 and 10.000 December 1963. The particle program included best estimates of sun and moon gravity, longitude-independent (zonal) earth gravity through fourth order, as well as triaxial earth gravity (associated with equatorial ellipticity).

On the basis of this validation, the actual drift of Syncom II over Brazil, as derived at Goddard Space Flight Center from range and range-rate radar and Minitrack observations covering a 7-month period in 1963-1964, is reduced by the theory to yield the following two parameters of the earth's equatorial ellipticity:

$$J_{22} = -(1.70 \pm 0.05) \times 10^{-6},$$

(representing a 65 ± 2 meter difference between major and minor equatorial radii); and

$$\lambda_{22} = -(19 \pm 6)^{\circ}$$

(locating the geographic longitude of the major equatorial axis). These results show a somewhat stronger and west-shifted equatorial ellipticity than recent geodetic investigations in 1963-1964 indicate.

Dulhoo

CONTENTS

DETERMINATION OF THE ELLIPTICITY OF THE EARTH'S EQUATOR FROM OBSERVATIONS ON THE DRIFT OF THE SYNCOM II SATELLITE

by
Carl A. Wagner
Goddard Space Flight Center

INTRODUCTION

Almost as soon as Syncom II, the world's first operational 24-hour satellite, was left alone to drift free in the gravity fields of the earth, sun, and moon high above the earth, it began to deviate noticeably from the predicted path. The principal observed effect, unexplained in the orbit-determination theory used for this satellite (which included all well-known solar, lunar, and earth-gravity effects), was a small but continual daily change of the semimajor axis. As a result of this secular drift anomaly, the elements for Syncom II (1963 31A) have undergone revision about every week since mid-summer 1963, to allow adequate tracking acquisition for the succeeding week.

The investigation reported herein was undertaken primarily as an attempt to explain as fully as possible the reasons for, and all the observed features of, this secular drift. Many possible causes were examined for order-of-magnitude effect and were rejected; these included magnetic field interactions, micrometeorite collision drag, and solar wind and radiation perturbations.* Outgassing from the satellite during the free drift periods starting in mid-August 1963 is believed to have been negligible. To have contributed to the observed steady secular increase of the semi-major axis, residual outgassing from the spin-stabilized satellite would have had to occur regularly at selective times in the rotation cycle—a highly unlikely series of events over many months of drift.

It was concluded that longitude-dependent earth gravity was the most likely cause of the long-term accelerated free drift of Syncom II. Significant longitude-dependent earth gravity will cause detectable perturbations of satellite orbits which can be appreciable over fairly short periods of time in special "Resonance" cases such as the 24-hour satellite (see Reference 1, for example).

*See Appendix F in Goddard Space Flight Center Document X-621-64-90, April 1964, by C. A. Wagner: "Determination of the Triaxiality of the Earth from Observations on the Drift of the Syncom II Satellite."

Summary of Previous Longitude-Dependent Earth-Gravity Investigations

The question of the existence and extent of the longitude dependence of the earth's gravity field has concerned geodesists since the early years of this century (see Reference 2, for example). The existence of a longitude-dependent field implies the existence of inhomogeneities and states of stress within the earth which are of fundamental importance to all dynamical theories of the earth's interior.

Table A1, Appendix A, summarizes 40 previous reductions of gravimetric, astrogeodetic, and satellite gravity data reporting longitude terms in the earth's external gravity field. It is quickly seen that, even though the more recent gravity reductions show closer agreement in term-by-term detail than the older ones, exact knowledge of tesseral earth gravity is still in its infancy—basically, because of the scarcity of good data over more than a small portion of the external field. Surface gravity data, prior to the recent use of accurate sea-going gravimeters, have been very scattered and often of dubious quality. Uncertainties in surface-station position with respect to the center of the earth's mass of the order of only 10 meters can cause serious errors in tesseral gravity reductions, since this is the order of magnitude of the geoid deviations caused by longitude-dependent gravity. In addition, scattered surface gravity data, unless smoothed with great care, tend to overemphasize the higher order tesseral terms of greater spatial frequency, because the gravimeter will be sensitive to the gravity distortion of even close-by mass anomalies. Satellite gravity reductions, inherently more insensitive to the higher order terms, have suffered most to date from being based on too limited a number of medium-altitude medium-inclination satellites. The chief result of this poor field sampling has been to make it difficult to separate the effects of individual tesseral terms of the same spatial frequency.

The situation does not seem as bad when the constants of the most recent tesseral gravity reductions are taken as a set and displayed cumulatively as deviations from a mean earth geoid (Appendix A, Figures A2 to A8). Still, as late as July 1963, Izsak stated (Reference 3), "It might be some time before one can arrive at definite conclusions regarding the longitude dependence of the earth's gravity field."

The use of 24-hour near-circular orbit satellites for geodetic purposes (as revealed in this investigation) has certain obvious advantages over lower altitude and surface data reductions. For the near-stationary satellite, any small-latitude symmetric earth-gravity anomaly in longitude will, in time, cause significant longitude drift of the ground track configuration which can be evaluated to high precision after a long period of observation. The great height of the 24-hour satellite makes it sensitive only to the very lowest orders of gravity anomalies, thus making it easier to separate out the effects of individual tesseral terms in the total field (see Appendix A, Figure A1 for example).

On the other hand, the great altitude of the 24-hour satellite has its drawbacks. The longitude perturbations to be sensed are extremely small at 24-hour altitudes: of the order of 10^{-7} of the earth's principal gravity attraction. The observation time for an accurate determination of this perturbation field must be long. Furthermore, the effect on the distant satellite of sun and moon

gravity over these long observation times cannot always be safely ignored, as it generally can for reductions from lower altitude satellite data.

In summary, it may be said that all earth satellites orbiting well above the atmosphere and below a level where sun and moon perturbations become too severe can be potentially useful in helping to clarify knowledge of the earth's actual gravity field. Twenty-four hour satellites appear ideally suited to defining individual components of this field to at least third order.

Purpose of Study

The author is not aware of an adequate presentation in the literature of the drift theory for an *inclined* 24-hour orbit satellite (such as Syncom II) in a longitude-dependent earth gravity field.

The purpose of this report, then, is threefold:

1. To present a theory for the drift of a 24-hour inclined satellite in a longitude-dependent earth-gravity field;
2. To interpret the actual drift of Syncom II (as assessed by a set of revised elements for the satellite) on the basis of this theory, thereby deriving measures of the longitude-dependent gravity field (i.e., shape of the geoid) which is assumed to be responsible for the observed drift;
3. To calculate maximum on-board station-keeping propulsion requirements for future 24-hour satellites based on the drift acceleration experience of Syncom II.

The measures of the earth's shape (geoid) derived in this report represent the first use of a 24-hour satellite for this purpose.

BASIC THEORY OF THE REDUCTION: ORBIT-AVERAGED DRIFT OF A 24-HOUR SATELLITE

(Determination of the Longitude Drift and Orbit Expansion for a 24-Hour Satellite in a Near-Circular Inclined Orbit Affected by a Small but Persistent Tangential Perturbing Force)

The dominant perturbations of a 24-hour equatorial satellite in a higher order earth-gravity field have been derived many times in the literature (References 1, 4, and 5).* In these references the perturbations were found by directly linearizing the equations of motion themselves and displaying the perturbed motion in appropriate geographic coordinates; no attempt was made to treat the drift of the *inclined* 24-hour satellite.

This report departs from the rather involved and difficult-to-visualize procedure of linearization of the equations of motion. Instead, it is shown how simply the dominant drift and orbit

*Also: Barrett, C. C., "The Perturbations of a Synchronous Satellite Resulting from the Gravitational Field of a Triaxial Earth," GSFC Document X-623-62-160, September 1962.
And: Private communication from R. H. Frick and T. B. Garber, 1962 (Rand Corp. Memo RM-2296).

expansion equations for the 24-hour satellite can be found by calculating the "perturbation of the two-body energy" of the geographically stationary satellite due to the small but persistent longitude-dependent earth-gravity force. This paper will not discuss in detail the limits of validity of the expressions derived, except in the case of the "inclination factor," which is discussed in Appendix B. To assess the accuracy with which these expressions predict the satellite's behavior, simulated trajectories with typical Syncom II orbit elements have been run on Goddard's particle program ITEM (Interplanetary Trajectory by an Encke Method). These trajectories (Appendix C) confirm the validity of the derived drift equations to an accuracy well within the "noise levels" in the orbital elements reported for Syncom II (Appendix D). The equations are essentially the same as those which Dr. Musen has derived (though not explicitly) by a more general but complex "energy perturbation" method (Reference 6).

In Figure 1, F is a small earth-gravity perturbation force acting tangentially to an initial circular 24-hour satellite orbit and ds is a small arc length of the satellite's path around the earth.* At the beginning of the dynamics, the total energy (the sum of potential and kinetic) of the satellite in a spherical earth-gravity field (Reference 7) is

$$E = -\frac{\mu_E}{2a_s}, \tag{1}$$

where μ_E is the earth's gaussian gravity constant (3.986×10^5 km^3/sec^2). The energy added to the satellite by F per day is

$$\Delta E = \oint F\,ds = 2\pi a_s \bar{F}, \tag{2}$$

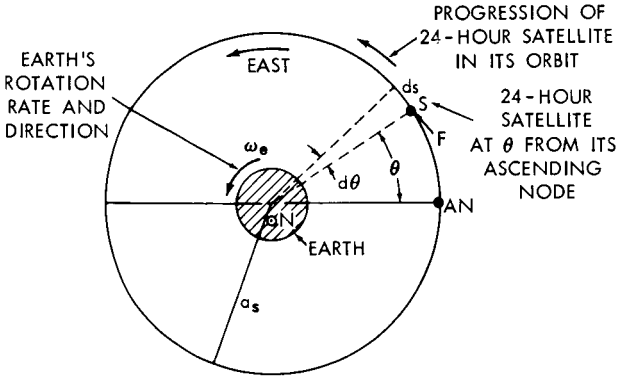

Figure 1—Orbit plane of a 24-hour satellite, looking southerly.

where $\bar{F} = (1/2\pi)\oint F\,d\theta$. In units of force per unit mass, $\bar{F}$ is the orbit-averaged energy perturbing force. If the orbit is purely circular, only a tangential perturbation force can cause a change in the total energy. The ITEM simulated trajectories in Appendix C and the real Syncom II orbits both maintain eccentricities of the order of 0.0001 for periods up to 100 days. Equation 2 assumes that the eccentricity is zero for the 24-hour satellite of semimajor axis a_s.

From Equation 1, the change in energy of a 24-hour satellite is accompanied by a change in

*Symbols used in this report are defined in Appendix F.

semimajor axis expressed by

$$\Delta E = \frac{\mu_E \Delta a_s}{2(a_s)^2} ,$$

or

$$\Delta a_s = \frac{2(a_s)^2 \Delta E}{\mu_E} . \tag{3}$$

Substituting Equation 2 into 3, the change in semimajor axis of the 24-hour near-circular orbit, per day, is approximately given by

$$\Delta a_s = \frac{4\pi (a_s)^3 \bar{F}}{\mu_E} . \tag{4}$$

From Kepler's third law, the period of a 24-hour orbit as a function of its semimajor axis is

$$T_s = \frac{2\pi (a_s)^{3/2}}{(\mu_E)^{1/2}} . \tag{5}$$

Thus, if the semimajor axis changes by Δa_s, the period change is given by

$$\Delta T_s = \frac{3\pi (a_s)^{1/2} \Delta a_s}{(\mu_E)^{1/2}} . \tag{6}$$

Substituting Equation 4 into 6, the change in period, per day, of a 24-hour circular orbit is given by

$$\Delta T_s = \frac{12\pi^2 (a_s)^{7/2} \bar{F}}{(\mu_E)^{3/2}} . \tag{7}$$

The apparent net longitudinal drift rate of the 24-hour satellite's ground track with respect to the surface of the earth (see Figure 3) after the first sidereal day is

$$\dot{\lambda}(t = 1 \text{ sid. day}) = - \frac{(\Delta T_s)\, 2\pi}{T_s} \text{ rad/sid. day.}^* \tag{8}$$

The minus sign is taken in Equation 8 because a gain in period is accompanied by a decrease in net geographic longitude for the initially 24-hour satellite (for example, for the daily geographic

*See Isley, W. C., "A summary of Constants Associated with Orbital Analysis of Earth Satellites, Including the Influence of their Uncertainties upon Gravitational Measurements for Synchronous Satellities," GSFC Document X-623-62-169, 1962.

position of the ascending equator crossing). Combining Equations 7 and 5 in 8 gives

$$\dot{\lambda}(t = 1 \text{ sid. day}) = -\frac{12\pi^2 \bar{F}}{\mu_E/(a_s)^2} \text{ rad/sid. day.} \tag{9}$$

As the gain in semimajor axis is small over one day (and, in fact, small compared with a_s for the entire libration period of the satellite in the triaxial earth field), the drift rate will continue to build up linearly with time initially, adding increments of Equation 9 each day. Thus, the net longitudinal drift acceleration of an initially 24-hour satellite is

$$\ddot{\lambda} = -\frac{12\pi^2 \bar{F}}{\mu_E/(a_s)^2} \text{ rad/sid. day}^2 . \tag{10}$$

For the equatorial synchronous satellite, F is a constant at every point in the orbit equal to the longitude perturbation force at that equatorial position. For this satellite, the drift acceleration as a function of λ (in a second-order gravity field) is simply given from Equation 10 as

$$\ddot{\lambda} = A_{22} \sin 2\left(\lambda - \lambda_{22}\right) \text{ rad/sid. day}^2, \tag{10a}$$

where

$$A_{22} \text{ (equatorial)} = -72\pi^2 J_{22} \left(R_0/a_s\right)^2 \text{ rad/sid. day}^2. \tag{10b}$$

(See next section and Appendix A, Equation A4.) Equation 10a has been derived by a more complex perturbation method.* Rewriting Equation 4 as

$$\dot{a} = \frac{4\pi (a_s)^3 \bar{F}}{\mu_E} \text{ length units/sid. day} \tag{11}$$

gives the expansion rate of the initially 24-hour near-circular satellite orbit due to a small but persistently acting orbit-averaged tangential perturbing force $\bar{F}$.

EVALUATION OF ORBIT-AVERAGED PERTURBING FORCE FOR AN INCLINED-ORBIT 24-HOUR SATELLITE

While the energy-changing force on the stationary equatorial satellite is constant over a single orbit, this is no longer true for the inclined 24-hour satellite. Such a circular orbit satellite describes a closed, narrow "figure 8" path over the earth's surface, centered on the equator (see Figure 3).

*Frick and Garber, *op. cit.* (See footnote, p. 3).

At each point on this path the tangential, energy-changing force is different, as both the longitude and latitude change during the daily excursion. This along-track force is now made up of contributions from both latitude and longitude gravity perturbation forces (Appendix A). It can be shown that the zonal gravity forces have no net daily energy effect on the circular inclined orbit. The net daily contributions from the latitude and longitude perturbation forces due to the earth's presumed elliptical equator are not zero. It turns out that the net contribution from the longitude perturbation dominates for orbits of small and medium inclination.

Figure 2 shows the position of the 24-hour satellite with respect to the earth and the celestial sphere. The earth-gravity perturbing forces in the radial, latitude, and longitude directions, F_r, F_ϕ, and F_λ, are assumed to be acting on the satellite at s.

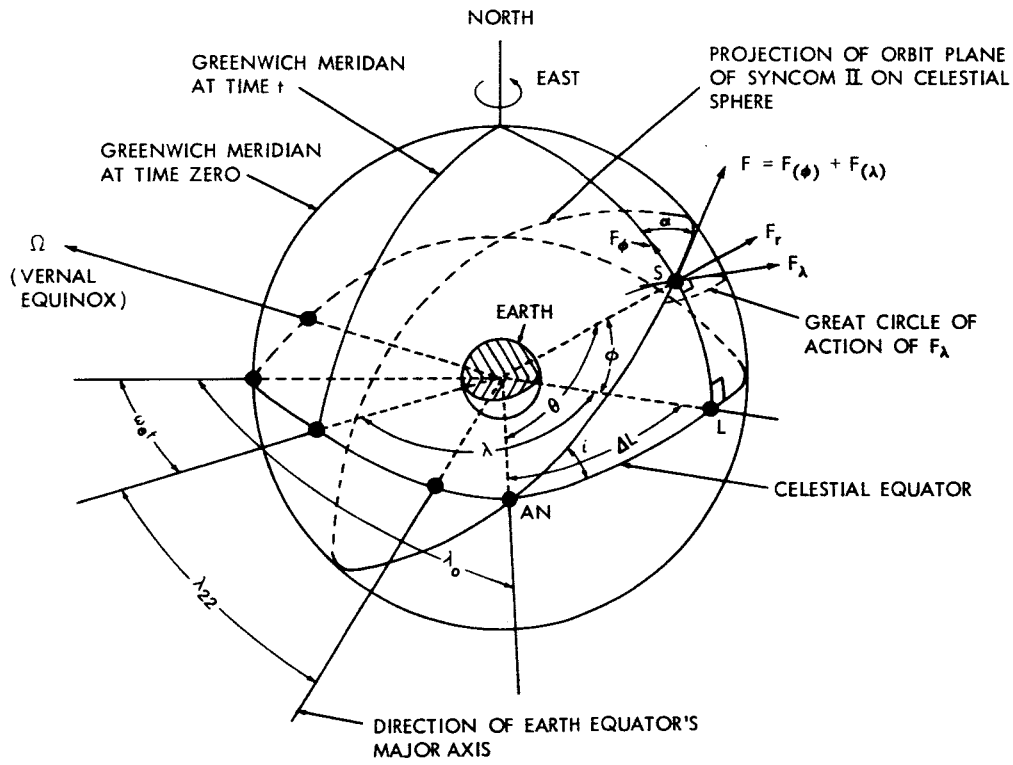

Figure 2—Position of a 24-hour satellite with a near-circular orbit with respect to the earth and the celestial sphere.

If only the earth-gravity perturbation forces arising from the ellipticity of the earth's equator are considered,* Appendix A gives these forces as

$$F_r = \frac{\mu_E \left(R_0/a_s\right)^2}{\left(a_s\right)^2} \left[9J_{22} \cos^2\phi \cos 2\left(\lambda - \lambda_{22}\right)\right] , \qquad (12)$$

*Wagner, C. A., "The Gravitational Potential of a Triaxial Earth," GSFC Document X-623-62-206, October 1962.

$$F_\phi = \frac{\mu_E \left(R_0/a_s\right)^2}{\left(a_s\right)^2} \left[6J_{22} \cos\phi \sin\phi \cos 2\left(\lambda - \lambda_{22}\right)\right] , \tag{12a}$$

$$F_\lambda = \frac{\mu_E \left(R_0/a_s\right)^2}{\left(a_s\right)^2} \left[6J_{22} \cos\phi \sin 2\left(\lambda - \lambda_{22}\right)\right] . \tag{13}$$

As long as the orbit is nearly circular, F_r will have negligible contribution to F. The contribution to F from F_ϕ is

$$F_{(\phi)} = F_\phi \cos\alpha = K \sin\phi \cos\phi \cos\alpha \cos 2\left(\lambda - \lambda_{22}\right) ; \tag{14}$$

K is a constant for a single orbit:

$$K = 6J_{22} \frac{\mu_E R_0^2}{\left(a_s\right)^4} . \tag{14a}$$

In the right spherical triangle AN, S, L note the following trigonometric relations:

$$\cos i = \frac{\tan\Delta L}{\tan\theta} , \tag{15a}$$

$$\cos\alpha = \frac{\tan\phi}{\tan\theta} , \tag{15b}$$

$$\sin\phi = \sin i \sin\theta , \tag{15c}$$

$$\sin\alpha = \frac{\cos i}{\cos\phi} . \tag{15d}$$

From Equation 15a,

$$\Delta L = \tan^{-1}(\tan\theta \cos i) . \tag{16}$$

Let the geographic longitude of the satellite at the ascending node AN be λ_0. If time is counted from this orbital position, the geographic longitude of the 24-hour satellite at s in its near-circular orbit is

$$\lambda = \lambda_0 + \Delta L - \omega_e t \quad \text{(Figure 2)} ;$$

or, using Equation 16,

$$\lambda = \lambda_0 + \tan^{-1}(\tan\theta \cos i) - \omega_e t ; \tag{17}$$

(ω_e is the earth's sidereal rotation rate). For the 24-hour satellite [starting the dynamics with S at AN (ascending node) for convenience], $\theta \doteq \omega_e t$, so that Equation 17 becomes

$$\lambda = \lambda_0 + \tan^{-1}(\tan\theta \cos i) - \theta \ , \tag{18}$$

approximately. The function $\tan^{-1}(\tan\theta \cos i) - \theta$ is "even" about $\theta = 0$ and $\theta = \pi/2$, with a period of π, and behaves like a somewhat distorted sine function (Figure 3 and Appendix B). Call this function $\Delta\lambda$ and note that, for $i < 33$ degrees, $\Delta\lambda$ is always less than 5 degrees. Thus, using Equation 18 and assuming i is sufficiently small ($i < 45$ degrees proves to be a sufficient restriction on the inclination), $\cos 2(\lambda - \lambda_{22})$ for the 24-hour satellite can be approximated by

$$\cos 2(\lambda - \lambda_{22}) \doteq \cos 2(\lambda_0 - \lambda_{22}) - 2\Delta\lambda \sin 2(\lambda_0 - \lambda_{22}) = -\cos 2\gamma_0 + 2\Delta\lambda \sin 2\gamma_0 \ . \tag{18a}$$

(Note that $\gamma_0 = 90° + \lambda_0 - \lambda_{22}$ from Figure 3.) Similarly, $\sin 2(\lambda - \lambda_{22})$ can be approximated by

$$\sin 2(\lambda_0 - \lambda_{22}) + 2\Delta\lambda \cos 2(\lambda_0 - \lambda_{22}) = -\sin 2\gamma_0 - 2\Delta\lambda \cos 2\gamma_0 \doteq \sin 2(\lambda - \lambda_{22}) \ . \tag{18b}$$

In Equations 18a and 18b, γ_0 is the geographic longitude of the node of the 24-hour near-circular satellite orbit with respect to the minor equatorial axis (Figure 3). With these expansions (Equations 18a and 18b), and using 15b, Equation 14 becomes

$$F_{(\phi)} = K \frac{\sin\phi \cos\phi \tan\phi}{\tan\theta} \left(-\cos 2\gamma_0 + 2\Delta\lambda \sin 2\gamma_0\right) \ .$$

Using Equation 15c in the above expression, the contribution to the perturbing force F due to F_ϕ becomes

$$F_{(\phi)} = K \frac{\sin^2 i \sin 2\theta}{2} \left(-\cos 2\gamma_0 + 2\Delta\lambda \sin 2\gamma_0\right) \ . \tag{19}$$

Writing $\Delta\lambda \doteq \Delta\lambda_{max} \sin 2\theta$, Equation 19 becomes

$$F_{(\phi)} \doteq K \sin^2 i \left(-\cos 2\gamma_0\right) \frac{\sin 2\theta}{2} - K \sin^2 i \, \Delta\lambda_{max} \left(\sin 2\gamma_0 \sin^2 2\theta\right) \ . \tag{20}$$

Averaging $F_{(\phi)}$ over $0 \leq \theta \leq 2\pi$, Equation 20 gives

$$\bar{F}_{(\phi)} = \frac{1}{2\pi} \int_0^{2\pi} F_{(\phi)} \, d\theta = -\frac{\sin^2 i \Delta\lambda_{max}}{2} (K \sin 2\gamma_0) \ . \tag{21}$$

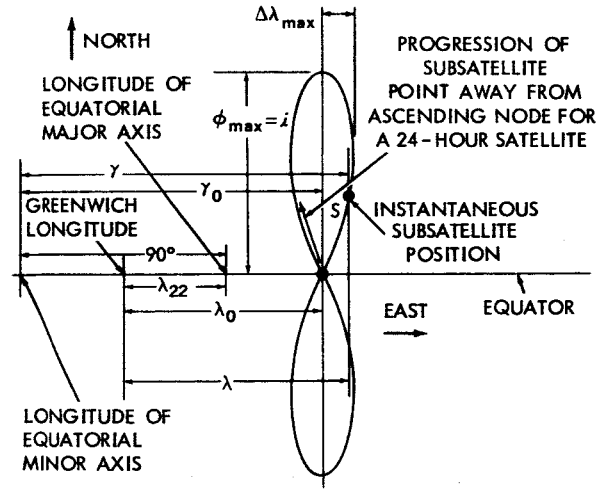

Figure 3—Geographic subsatellite track of a 24-hour satellite in a near-circular orbit.

The contribution to F from F_λ is

$$F_{(\lambda)} = F_\lambda \cos(90° - \alpha) = F_\lambda \sin\alpha = K \sin\alpha \cos\phi \left(-\sin 2\gamma_0 - 2\Delta\lambda \cos 2\gamma_0\right) , \tag{22}$$

from Equations 13 and 18b. Using Equation 15d in 22 and noting that $\Delta\lambda \doteq -\Delta\lambda_{max} \sin 2\theta$, as before, gives the contribution to F from F_λ as

$$F_{(\lambda)} = K \cos i \left[-\sin 2\gamma_0 + 2\Delta\lambda_{max} \sin 2\theta \cos 2\gamma_0\right] . \tag{23}$$

Averaging $F_{(\lambda)}$ over $0 \leq \theta \leq 2\pi$, Equation 23 gives

$$\bar{F}_{(\lambda)} = -K \cos i \sin 2\gamma_0 . \tag{24}$$

Thus, combining the contributions of the latitude and longitude perturbations to the average perturbation force over a single 24-hour orbit, Equations 21 and 24 sum to produce

$$\bar{F}_{total} = \bar{F}_{(\phi)} + \bar{F}_{(\lambda)} = -K \sin 2\gamma_0 \left[\cos i + \frac{\sin^2 i \, \Delta\lambda_{max}}{2}\right]. \tag{25}$$

COMPLETION OF DERIVATION OF DRIFT EQUATIONS FOR A 24-HOUR SATELLITE

Appendix B shows that

$$\Delta\lambda_{max} = \tan^{-1}(\sec i) - 45 \text{ degrees} .$$

It is also shown there that, to a high degree of accuracy for $i < 50$ degrees,

$$\cos i + \frac{\sin^2 \Delta\lambda_{max}}{2} \doteq \frac{1 + \cos^2 i}{2} .$$

Numerically integrated orbits have shown that the drift theory for a 24-hour satellite stemming from Equation 25 is in error by more than 2 percent for $i > 45$ degrees. With this restriction in orbit inclination, using the above approximation for the inclination factor, we can rewrite the longitude drift and orbit expansion equations (10 and 11), evaluating $\bar{F}$ by Equation 25, giving

$$\ddot{\gamma}_0 = \frac{12\pi^2 K}{\mu_E / (a_s)^2} \left(\frac{\cos^2 i + 1}{2}\right) \sin 2\gamma_0 \text{ rad/sid. day}^2 \tag{26}$$

(where $\ddot{\gamma}_0$ refers to the net acceleration of the initial ascending equator crossing longitude γ_0) and

$$\dot{a} = -\frac{4\pi (a_s)^3 K}{\mu_E} \left(\frac{\cos^2 i + 1}{2}\right) \sin 2\gamma_0 \text{ length units/sid. day} . \tag{27}$$

Substituting Equation 14a into 26 and 27 reduces these expressions to

$$\ddot{\gamma}_0 = 72\pi^2 J_{22} \left(R_0/a_s\right)^2 \left(\frac{\cos^2 i + 1}{2}\right) \sin 2\gamma_0 \quad \text{rad/sid. day}^2 \tag{28}$$

and

$$\dot{a} = -24\pi J_{22} \left(R_0/a_s\right) R_0 \left(\frac{\cos^2 i + 1}{2}\right) \sin 2\gamma_0 \quad \text{length units/sid. day} . \tag{29}$$

Define a nondimensional change of semimajor axis from a_s during the drift as

$$a_1 = \frac{a - a_s}{a_s} = \frac{\Delta a}{a_s} , \text{ so that } \dot{a}_1 = \frac{\dot{a}}{a_s} . \tag{29a}$$

With Equation 29a, Equation 29 becomes

$$\dot{a}_1 = -24\pi J_{22} \left(R_0/a_s\right)^2 \left[\frac{\cos^2 i + 1}{2}\right] \sin 2\gamma_0 , \ 1/\text{sid. day} . \tag{30}$$

Define

$$A_{22} = -72\pi^2 J_{22} \left(R_0/a_s\right)^2 \left[\frac{\cos^2 i + 1}{2}\right] \text{rad/sid. day}^2 . \tag{30a}$$

With Equation 30a, Equations 28 and 30 become

$$\ddot{\gamma}_0 + A_{22} \sin 2\gamma_0 = 0 \quad \text{rad/sid. day}^2 \tag{31}$$

and

$$\dot{a}_1 - \frac{A_{22} \sin 2\gamma_0}{3\pi} = 0 , \ 1/\text{sid. day} . \tag{32}$$

The long-term drift regime for the 24-hour inclined-orbit satellite (as described by Equations 31, 32, and 30a) is thus the same as for the equatorial satellite* modified only by the inclination factor $\left(\cos^2 i + 1\right)/2$.

Note that π in Equation 32 has dimensions of radians per sidereal day. It must be understood that Equation 31 describes the *net* daily geographic acceleration of the initially 24-hour satellite with respect to the earth's minor equatorial axis. Stated another way, Equation 31 describes the geographic drift of the entire originally stationary, figure-8 ground track (Figure 3). Similarly,

*See: Frick and Garber, *op. cit.* and Barrett, *op. cit.* (footnote, p. 3).

Equation 32 describes the net daily orbit-expansion rate of the 24-hour satellite. In particular, it is convenient to treat the motion of the ascending node of the orbit in geographic longitude as a reference for the entire configuration. In what follows, therefore, γ will refer always to the geographic longitude of the ascending equator crossing east of the equatorial minor axis and γ_0 will refer to the initial geographic longitude of the ascending equator crossing east of the minor axis, at the start of the dynamics under consideration. Equations 31 and 32 can thus be rewritten in terms of the general ascending equator crossing longitude position γ, to give the relevant partially uncoupled long-term drift and orbit-expansion differential equations for the near-24-hour near-circular orbit satellite:

$$\ddot{\gamma} + A_{22} \sin 2\gamma = 0 \quad \text{rad/sid. day}^2 \tag{33}$$

and

$$\dot{a}_1 - \frac{A_{22} \sin 2\gamma}{3\pi} = 0 \ , \quad 1/\text{sid. day} \tag{34}$$

GENERAL CONSIDERATIONS OF SOLUTIONS OF DRIFT EQUATIONS: LIBRATORY DRIFT REGIME OF AN INCLINED-ORBIT 24-HOUR SATELLITE

Equation 33 can be integrated directly for the geographic drift rate by noting that

$$\ddot{\gamma} = \frac{d\dot{\gamma}}{dt} = \frac{d\dot{\gamma}^2}{2\dot{\gamma}\, dt} = \frac{d\dot{\gamma}^2}{2d\gamma} \ .$$

Thus, Equation 33 can be separated to

$$d\dot{\gamma}^2 = -2A_{22} \sin 2\gamma \, d\gamma \ . \tag{35}$$

Since the variables $\dot{\gamma}^2$ and γ are separated in Equation 35, this equation integrates to

$$\dot{\gamma}^2 = A_{22} \cos 2\gamma + C_1 \ . \tag{36}$$

With the initial condition that $\dot{\gamma} = \dot{\gamma}_0$ at $\gamma = \gamma_0$, Equation 36 becomes

$$\dot{\gamma} = \left[(\dot{\gamma}_0)^2 + A_{22} \left(\cos 2\gamma - \cos 2\gamma_0 \right) \right]^{1/2} \ , \tag{37}$$

giving the drift rate of the 24-hour satellite as a function of the initial drift rate $\dot{\gamma}_0$, the earth-gravity constant A_{22}, the initial longitude east of the minor axis γ_0, and the instantaneous longitude γ. Returning to the semicoupled system of Equations 33 and 34, the explicit dependence of the equations on the location from the minor axis and the magnitude of the equatorial ellipticity may be eliminated by multiplying Equation 33 by $1/3\pi$ and adding the resulting equation to 34, giving

$$\ddot{\gamma} + 3\pi \dot{a}_1 = 0 \ . \tag{38}$$

Equation 38 can be rewritten as

$$\frac{d\dot{\gamma}}{dt} + 3\pi \dot{a}_1 = 0 = d\dot{\gamma} + 3\pi \dot{a}_1 \, dt = d\dot{\gamma} + 3\pi \, d a_1 \, . \tag{39}$$

Separation of the variables $\dot{\gamma}$ and a_1 is thus achieved in Equation 39, which integrates directly to

$$3\pi a_1 + \dot{\gamma} = C_2 \, . \tag{40}$$

With the initial conditions, $a_1 = 0$ when $\dot{\gamma} = 0$ (or the satellite is in the momentarily stationary ground-track configuration), the integration constant C_2 is evaluated as 0. If γ_0 in Equation 37 is also the longitude of this initially stationary orbit, $(\dot{\gamma}_0)^2 = 0$ there, and Equation 37 in 40 yields for a_1, the semimajor axis change from "synchronism" in the drift motion,

$$a_1 = \pm \frac{(A_{22})^{1/2} (\cos 2\gamma - \cos 2\gamma_0)^{1/2}}{3\pi} \, . \tag{41}$$

Equation 41 shows explicitly that the semimajor axis is bounded in long-term drift from a stationary orbit. From Equation 33, since $A_{22} > 0$, if $0 < \gamma_0 < 90$ degrees, drift proceeds *toward* the nearest longitude of the earth's equatorial minor axis (in the $-\gamma$ direction). If -90 degrees $< \gamma_0 < 0$ degrees, then 33 shows that drift again proceeds *toward* the nearest minor axis longitude (in the $+\gamma$ direction). Thus, in all cases of drift from a stationary geographic configuration, $\cos 2\gamma - \cos 2\gamma_0$ is a positive function which has a maximum when $\gamma = 0$ (when the satellite has drifted over the longitude of the minor axis). Thus Equation 41 gives (for the librations of a 24-hour satellite)

$$a_{1,max} = \left| \frac{(A_{22})^{1/2} (1 - \cos 2\gamma_0)^{1/2}}{3\pi} \right| \, . \tag{42}$$

Again, it is noted that π in Equation 42 has units of radians per sidereal day. An absolute maximum semimajor axis change in the drift occurs when the "synchronous" condition is established near the longitude of the major equatorial axis. Here, $\gamma_0 = -90$ degrees, $\cos 2\gamma_0 = -1$, and

$$a_1 \text{ (absolute maximum for a librating 24-hour satellite)} = \frac{(2A_{22})^{1/2}}{3\pi} \, . \tag{43}$$

For the constant $J_{22} = -1.7 \times 10^{-6}$ (derived in this study from long-term observations on the drift of the Syncom II satellite) and using the additional constants from this study ($i = 33$ degrees, $a_s \doteq 42166$ km, $R_0 = 6378.388$ km), Equation 30a gives

$$A_{22} = 23.2 \times 10^{-6} \text{ rad/sid. day}^2 \, .$$

Equation 43 then gives

$$a_1 \text{ (absolute max.)} = 0.72 \times 10^{-3}$$

from which, by Equation 29a,

$$\Delta a \text{ (absolute max. from a "synchronous" condition near the equatorial major axis, for a satellite of } i = 33 \text{ degrees)} = 30.7 \text{ km.}$$

Thus the assumption made in Equations 10 and 11, to approximate the slightly varying semimajor axis by a_s (a constant) throughout the drift motion, appears amply justified.

Figure 4 is a graph of Equation 41 for a_1 vs. γ (the longitude with respect to the nearest minor axis location) as a function of γ_0, the longitude in the initially stationary configuration.

Note that Equation 41 allows equal ± values for a_1 for each γ. Suppose the satellite is initially at $+\gamma_0$ (position 1 in Figure 4) from the nearest location of the minor axis. From Equation 33, $\sin 2\gamma_0$ being positive, the satellite begins to drift west (attaining a negative drift rate) toward the minor axis. But, from Equation 40, since $C_2 = 0$, $a_1 = -\dot{\gamma}/3n > 0$; the drift therefore proceeds counterclockwise in Figure 4, around the central point of the minor axis and $a_1 = 0$, along the upper portion of the two-valued arc determined from Equation 41.

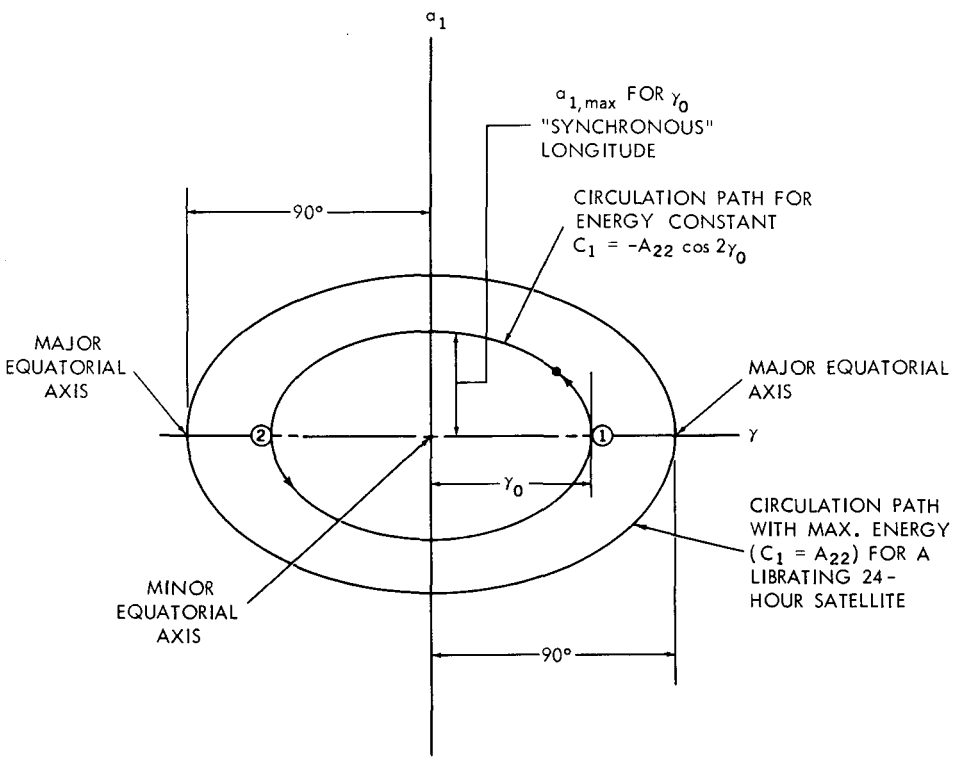

Figure 4—Libration with longitude of the semimajor axis of a 24-hour satellite as a function of the longitude of the initially stationary configuration.

The same situation holds for the motion beginning or stemming away from the "synchronous" longitude at $-\gamma_0$, position 2 in Figure 4. Here $\sin 2\gamma_0$ is negative, and the drift proceeds at a positive rate to the east. Again from Equation 40, as soon as the satellite leaves position 2, $a_1 = -\dot{\gamma}/3n < 0$, and the circulation continues in a counterclockwise direction. Every trajectory in the phase plane $a_1 \Leftrightarrow \gamma$ may be conveniently defined by the constant C_1 of the "energy integral" of the drift motion (Equation 36). Since Equation 33 is the equation of motion defining the large-angle oscillations of a mathematical pendulum (in the case of the 24-hour-orbit satellite, the point of symmetry is the minor axis where $2\gamma = 0$), it can be expected that the general solutions in that theory (Appendix E) apply to a good approximation to the long-term librations of the near-synchronous satellite, provided the drift rates are not large.* For example, in Equation 36, with a momentarily "synchronous" condition at γ_0 being given by $\dot{\gamma}_0 = 0$, the "energy constant" is evaluated as

$$C_1 = -A_{22} \cos 2\gamma_0 \ .$$

With this evaluation, Equation 36 becomes

$$\dot{\gamma}^2 - A_{22} \cos 2\gamma = -A_{22} \cos 2\gamma_0 \ . \tag{44}$$

Solving for the initially "synchronous" longitude as a function of any longitude in the drift and the corresponding longitude rate, Equation 44 gives

$$\gamma_0 = \frac{1}{2} \cos^{-1} \left(\cos 2\gamma - \frac{\dot{\gamma}^2}{A_{22}} \right) \cdot \tag{45}$$

Since $\dot{\gamma}^2/A_{22} \geq 0$, the argument of $\cos^{-1}$ in Equation 45 is always less than or equal to 1. Thus, as long as $\left(\cos 2\gamma - \dot{\gamma}^2\right)/A_{22} \geq -1$, then 45 will give a real solution for the momentarily "synchronous" longitude with respect to the minor axis. But, if $\left(\cos 2\gamma - \dot{\gamma}^2\right)/A_{22} < -1$, there will be no real momentarily "synchronous" configuration for the near-24-hour satellite. With this energy, the world-circulation regime commences, corresponding to the over-the-top, high-energy regime of the mathematical pendulum (Reference 1). The above inequality implies that, for the commencement of "world circulation" for the near-24-hour satellite,

$$\dot{\gamma}^2 \geq A_{22} \left(1 + \cos 2\gamma\right) \ ,$$

or

$$\dot{\gamma}^2 \geq 2A_{22} \cos^2 \gamma \ . \tag{46}$$

When $2\gamma = 0$, or the satellite is over the minor axis, Equation 46 allows the maximum possible drift rate for a librating 24-hour satellite:

$$\dot{\gamma}_{\text{max, for libration}} = \left(2A_{22}\right)^{1/2} \text{ rad/sid. day} \ . \tag{47}$$

*Author has two papers "in preparation, 1965" on this subject, to be Goddard Space Flight Center X-documents.

For example, using the reported value of $A_{22} = 23.2 \times 10^{-6}$ rad/sid. day^2 for the inclination of the Syncom II satellite, Equation 47 gives

$$\dot{\gamma}_{\text{max, for libration with } J_{22} = -1.7 \times 10^{-6},\ i = 33^\circ} = \left(46.4 \times 10^{-6}\right)^{1/2} \approx 0.39 \text{ degree/day.} \tag{48}$$

APPROXIMATIONS TO EXACT DRIFT SOLUTIONS FOR PERIODS VERY CLOSE TO SYNCHRONOUS

Although a first integral to Equation 33 can be found easily (Appendix E), the second integral can give the drift only as a function of time in a closed form, in terms of an elliptic function. However, for reasonably small excursions from a momentarily synchronous configuration, Appendix E shows that the elliptic function can be approximated to good accuracy by the first few terms of a Taylor series expansion in the time from synchronism Δt.

Expanding the drift from the "synchronous" longitude ($\gamma = \gamma_0$ in this section) in a Taylor series, with respect to increments of time Δt from the momentarily stationary condition,

$$\gamma(\Delta t) = \gamma_0 + \dot{\gamma}_0 \Delta t + \ddot{\gamma}_0 \frac{(\Delta t)^2}{2} + \dddot{\gamma}_0 \frac{(\Delta t)^3}{6} + \gamma_0^{[4]} \frac{(\Delta t)^4}{24}$$

$$+ \gamma_0^{[5]} \frac{(\Delta t)^5}{120} + \gamma_0^{[6]} \frac{(\Delta t)^6}{720} + \gamma_0^{[7]} \frac{(\Delta t)^7}{5040} + \gamma_0^{[8]} \frac{(\Delta t)^8}{40320} + \cdots . \tag{49}$$

Differentiating Equation 33 six times with respect to time, it is clear that all derivatives in Equation 49 can be written as functions of A_{22}, γ_0, and $\dot{\gamma}_0$. Noting that $\gamma(\Delta t) - \gamma_0 = \Delta\lambda$ (the geographic longitude with respect to the "synchronous" configuration) and $\dot{\gamma}_0 = 0$, then 49 can be shown to reduce to the expansion

$$\Delta\lambda = \left(-A_{22} \sin 2\gamma_0\right) \frac{(\Delta t)^2}{2} + \left[\left(A_{22}\right)^2 \sin 4\gamma_0\right] \frac{(\Delta t)^4}{24} + \left[\left(A_{22}\right)^3 \sin 2\gamma_0 \left(4 \sin^2 2\gamma_0 - 1\right)\right] \frac{(\Delta t)^6}{180}$$

$$- \left[\left(A_{22}\right)^4 \sin 4\gamma_0 \left(34 \sin^2 2\gamma_0 - 1\right)\right] \frac{(\Delta t)^8}{10080} + \cdots . \tag{50}$$

It is apparent that, as $\Delta t \to 0$, the higher order terms of Equation 50 become increasingly more insignificant to the total drift, in comparison to the terms of lower order.

In Appendix E, the exact "elliptic integral" of motion from Equation 33 is calculated from a synchronous longitude of 60 degrees east of the minor axis. This calculation demonstrates that the simple term-inclusion-time criterion below gives an adequately converging series to the "exact" drift. In the actual reduction, all higher order terms in Equation 50 which are less in magnitude than the root mean square (rms) error of the observed Syncom II longitudes are ignored. The section on reduction of orbits (p. 22) in this report shows that this rms error of longitude determination for the ascending equator crossings of Syncom II from August 1963 to March 1964 has

been of the order of ±0.025 degree. Thus, 0.025 degree is used below in forming the minimum-time-term-inclusion criterion for each term of Equation 50. A_{22} is assumed to be 23.2×10^{-6} rad/sid. day^2.

1. For inclusion of the $(\Delta t)^4$ term,

$$\left|\sin 4\gamma_0\right| \text{ is maximum when } \gamma_0 = \pm 22.5 \text{ and } \pm 67.5 \text{ degrees.}$$

Therefore,

$$\left|\Delta\lambda_{max} \text{ (from the fourth-order term)}\right| = \left(A_{22}\right)^2 \frac{(\Delta t)^4}{24} . \tag{51a}$$

Solving Equation 51a for Δt, when $\left|\Delta\lambda_{max} \text{(fourth order)}\right| = 0.025$ degree,

$$\Delta t \text{ (min. fourth-order term inclusion)} = \left[0.025 \times 24/57.3 \times \left(23.2 \times 10^{-6}\right)^2\right]^{1/4}$$

$$= 66.5 \text{ sid. days from "synchronism."}$$

2. For inclusion of the $(\Delta t)^6$ term,

$$\left|\sin 2\gamma_0 \left(4 \sin^2 2\gamma_0 - 1\right)\right| \text{ is maximum when } \gamma_0 = \pm 45 \text{ degrees.}$$

Therefore,

$$\left|\Delta\lambda_{max} \text{ (from the sixth-order term)}\right| = \left(A_{22}\right)^3 \frac{(\Delta t)^6}{60} . \tag{51b}$$

Solving Equation 51b for Δt, when $\left|\Delta\lambda_{max} \text{ (sixth order)}\right| = 0.025$ degree,

$$\Delta t \text{ (min. for sixth-order term inclusion)} = \left[0.025 \times 60/57.3 \times \left(23.2 \times 10^{-6}\right)^3\right]^{1/6}$$

$$= 113 \text{ sid. days from "synchronism."}$$

3. For inclusion of the $(\Delta t)^8$ term,

$$\left|\sin^4 \gamma_0 \left(34 \sin^2 2\gamma_0 - 1\right)\right| \text{ is maximum when } \gamma_0 = \pm 59\ 1/4 \text{ degrees.}$$

Therefore,

$$\left|\Delta\lambda_{max} \text{ (from the eighth-order term)}\right| = 21.2 \left(A_{22}\right)^4 \frac{(\Delta t)^8}{10080} . \tag{51c}$$

Solving Equation 51c for Δt, when $\left|\Delta\lambda_{max}\ \text{(eighth order)}\right| = 0.025$ degree,

$$\Delta t\ \text{(min. for eighth-order term inclusion)} = \left[10080 \times 0.025/21.2 \times 57.3 \times \left(23.2 \times 10^{-6}\right)^4\right]^{1/8}$$

$$= 171\ \text{sid. days from "synchronism."}$$

Similarly, expanding $a_1(t)$ in a Taylor series about the time of "synchronism" (t_0, γ_0),

$$a_1\left(t_0 + \Delta t\right) = \left(a_1\right)_0 + \left(\dot{a}_1\right)_0 (\Delta t) + \left(\ddot{a}_1\right)_0 \frac{(\Delta t)^2}{2} + \left(\dddot{a}_1\right)_0 \frac{(\Delta t)^3}{6} + \cdots \quad . \tag{52}$$

But, from Equation 34,

$$\left(\dot{a}_1\right)_0 = \frac{A_{22} \sin 2\gamma_0}{3\pi} \quad . \tag{52a}$$

Differentiating Equation 52a with respect to time gives

$$\left(\ddot{a}_1\right)_0 = \frac{2\dot{\gamma}_0 A_{22} \cos 2\gamma_0}{3\pi} = 0 \ , \tag{52b}$$

since $\dot{\gamma}_0 = 0$. Differentiating Equation 52b with respect to time gives

$$\left(\dddot{a}_1\right)_0 = \frac{-4\left(\dot{\gamma}_0\right)^2 A_{22} \sin 2\gamma_0}{3\pi} + \frac{2\ddot{\gamma}_0 A_{22} \cos 2\gamma_0}{3\pi} = \frac{-\left(A_{22}\right)^2 \sin 4\gamma_0}{3\pi} \ , \tag{53}$$

using Equation 33. From the conventional definition of a_1, $\left(a_1\right)_0 = 0$. Equation 52 then becomes

$$a_1\ \text{(at } \Delta t \text{ from "synchronism")} = \frac{\left(A_{22} \sin 2\gamma_0\right)\Delta t}{3\pi} - \frac{\left(A_{22}\right)^2 \sin 4\gamma_0\ (\Delta t)^3}{18\pi} + \cdots \ , \tag{53a}$$

with the results of Equations 52a, 52b, and 53 in 52.

The section on reduction of orbits shows that the rms error of semimajor axis determination for Syncom II (including sun and moon "noise") is the order of ±0.5 km. Therefore, the rms error to be expected in a_1 is of the order of $0.5/42166 = 1.185 \times 10^{-5}$. Following the procedure for the longitude drift, 1.185×10^{-5} is used below to determine the minimum time for the inclusion of the terms beyond the first on the right-hand side of Equation 53a, to insure adequate convergence of the infinite series for $a_1(\Delta t)$.

1. For inclusion of the $(\Delta t)^3$ term,

$$\left|\sin 4\gamma_0\right| \text{ is maximum when } \gamma_0 = \pm 22.5 \text{ and } \pm 67.5 \text{ degrees.}$$

Therefore,

$$\left|a_{1,max} \text{ (from the third-order term of 53a)}\right| = \frac{(A_{22})^2 (\Delta t)^3}{18\pi} \cdot \tag{54}$$

Solving Equation 54 for Δt, when $\left|a_{1,max}\right| = 1.185 \times 10^{-5}$,

$$\Delta t \text{ (min. for the third-order term inclusion in 53a)} = \left(\frac{1.185 \times 10^{-5} \times 18\pi}{(23.2)^2 \times 10^{-12}}\right)^{1/3}$$

$$= 108 \text{ sid. days from synchronism.}$$

From a "synchronous" configuration at 54.8 degrees west of Greenwich, on or about September 6, 1963, Syncom II drifted to 59.2 degrees west of Greenwich on November 28, 1963, where it was "stopped" by the tangential firing of on-board cold-gas jets. A second free-drift period followed from a "synchronous" configuration at 59.2 degrees west on about November 29, 1963, to 66.3 degrees west on March 18, 1964, where the on-board tangential jets were fired to speed up the westward drift. Of the 34 separate orbits calculated by the Goddard Data and Tracking Systems Directorate for these free-drift periods, only 7 fell outside the minimum 66-day period around a condition of "synchronism," for which the inclusion of higher order terms in Equation 50 would be necessary in reducing the drift data according to that theory. The data reduction in the section on reduction of orbits includes only those orbits falling within the minimum 66-day period around "synchronism." Further refinement of this reduction to include the 7 outside-of-synchronous orbits (according to the above criterion) will be made in the near future. This refinement is not expected to materially affect the results of this report.

Summarizing, the results show that within reasonable excursions, the drift in longitude from a synchronous mean longitude is given approximately but explicitly in terms of time as

$$\lambda = \lambda_0 - \left(A_{22} \sin 2\gamma_0\right) \frac{\Delta t^2}{2} \cdot \tag{54a}$$

The corresponding mean daily radial drift is

$$a_1 = \left(\frac{A_{22} \sin 2\gamma_0}{3\pi}\right) \Delta t \ . \tag{54b}$$

Appendix E shows that Equations 54a and 54b are good approximations of the actual drift solutions if Δt is limited to the order of about 100 days for the probable order of magnitude of the earth's dominant tesseral gravity harmonic. The study in Reference 4 comes to the same conclusion. It is clear that the two drift periods for Syncom II, August to November 1963 and December to March 1963-1964, in the close neighborhood of momentary synchronism at 54.8°W and 59.2°W fulfill in large measure the requirements for accuracy of the explicit drift equations 54a and 54b. The actual analysis of the data relied most heavily on 54a, since the mean daily change of the semimajor

axis was more difficult to extract from the limited data because of sun and moon perturbations which had large variable effects on orbits with epochs at different anomalies from the ascending node of the satellite. Note that Equation 54a, differentiated twice, yields

$$\ddot{\lambda} = \ddot{\gamma} = -A_{22} \sin 2\gamma_0 \ , \tag{54c}$$

which is sufficiently accurate for the greater part of the two separate drift periods for Syncom II (see Appendix E). Thus, knowing $\ddot{\lambda}$ from the actual data for the two drift periods, Equation 54c can be solved uniquely for A_{22} and γ_0, giving the magnitude and phase angle of earth equatorial ellipticity assumed to have caused the accelerated drifts in the vicinity of the two separated "synchronous" longitudes.

DETERMINATION OF EARTH-EQUATORIAL ELLIPTICITY FROM TWO OBSERVATIONS OF DRIFT ACCELERATION AT A GIVEN LONGITUDE SEPARATION

While it is true that two evaluations of the near-synchronous drift accelerations at separated longitudes will determine the amplitude $(A_{22}$, and thus $J_{22})$ of the perturbing sine function, the phase angle $(\gamma_0$, and thus $\lambda_{22})$ will have multiple solutions. However, since it is known from the section on solutions of drift equations that the drift acceleration is always in the direction of the *nearest* extension of the *minor* equatorial axis of the earth, the proper quadrant of the phase angle of equatorial ellipticity always can be resolved.

Given two independent near-synchronous drifts (in the sense discussed previously), whose momentarily synchronous longitudes $(\gamma_0)_1$ and $(\gamma_0)_2$ are separated by $\nabla\lambda$. Let the two drift accelerations at these two "synchronous" configurations be $(\ddot{\gamma}_0)_1$ and $(\ddot{\gamma}_0)_2$. The drift accelerations may be determined from drift-data reduction according to the theory of Equation 50. From Equation 33,

$$(\ddot{\gamma}_0)_1 = -(A_{22})_1 \sin 2(\gamma_0)_1 \tag{55}$$

and

$$(\ddot{\gamma}_0)_2 = -(A_{22})_2 \sin 2\left[(\gamma_0)_1 + \nabla\lambda\right] \ , \tag{56}$$

since $(\gamma_0)_2 - (\gamma_0)_1 = \nabla\lambda = (\lambda_0)_2 - (\lambda_0)_1$. Expanding Equation 56 and dividing by 55 gives

$$\left[\frac{(\ddot{\gamma}_0)_2}{(\ddot{\gamma}_0)_1}\right]\left[\frac{(A_{22})_1}{(A_{22})_2}\right] = \left[\cos 2\nabla\lambda + \sin 2\nabla\lambda \cot 2(\gamma_0)_1\right] \ . \tag{57}$$

Solving Equation 57 for $(\gamma_0)_1$,

$$(\gamma_0)_1 = \frac{1}{2}\tan^{-1}\left[\frac{\sin 2\nabla\lambda}{\frac{(\ddot{\gamma}_0)_2 (A_{22})_1}{(\ddot{\gamma}_0)_1 (A_{22})_2} - \cos 2\nabla\lambda}\right] . \tag{58}$$

The quadrant of $(\gamma_0)_1$ is either the first or the fourth, because drift acceleration is always in the direction of the *nearest* longitude extension of the earth's *minor* equatorial axis.* Once the minor axis is located by Equation 58, the absolute value of J_{22} in the earth's triaxial gravity field can be determined through Equations 55 and 30a, for example, as

$$J_{22} = \frac{(A_{22})_1}{72\pi^2 \left[R_0/(a_s)_1\right]^2 \frac{\cos^2 i_1 + 1}{2}} = \frac{(\ddot{\gamma}_0)_1}{72\pi^2 \sin 2(\gamma_0)_1 \left[R_0/(a_s)_1\right]^2 \frac{\cos^2 i_1 + 1}{2}} . \tag{59}$$

Note that the units of $(\ddot{\gamma}_0)_1$ in Equation 59 must be those of radians per sidereal day^2, so that J_{22} will be dimensionless. Note also that in Equation 58, using the result of 30a,

$$\frac{(A_{22})_1}{(A_{22})_2} = \left[\frac{(a_s)_2}{(a_s)_1}\right]^2 \frac{\cos^2 i_1 + 1}{\cos^2 i_2 + 1} . \tag{60}$$

Using Equation 58, since $(\lambda_0)_1$ is known from the data reduction (the geographic longitude of the "synchronous" configuration), the geographic longitude of the nearest minor axis location can be calculated as

$$\gamma_{22} = (\lambda_0)_1 - (\gamma_0)_1 . \tag{60a}$$

Similarly, the geographic longitude of the nearest major equatorial axis location can be calculated from

$$\lambda_{22} = (\lambda_0)_1 - (\gamma_0)_1 + 90 \text{ degrees} \tag{60b}$$

(see Figure 3).

Following the theory of Wagner,† the difference in major and minor equatorial radii of the earth's triaxial geoid $a_0 - b_0$ is related to the gravity constant J_{22} by

$$a_0 - b_0 = -6R_0 J_{22} . \tag{61}$$

*Thus, the quadrant of the $\tan^{-1}$ in Eq. 58 can be most simply resolved by choosing the first or second quadrants if $(\ddot{\gamma}_0)_1 < 0$, and the third or fourth if $(\ddot{\gamma}_0)_1 > 0$.

†Wagner, *op. cit.* (See footnote, p. 7).

REDUCTION OF 27 SYNCOM II ORBITS TO DETERMINE THE EARTH'S EQUATORIAL ELLIPTICITY

Appendix D tabulates the 27 Syncom II orbits from which the reduction below was made. Table 1 gives the estimated ascending equator crossings nearest to the epoch of these orbits. These were calculated by hand and therefore are listed only to 0.01 degree and 0.01 day. The technique used was to locate from the Nautical Almanac the geographic longitude of the ascending node at epoch through the reported right ascension of the ascending node for the orbit, and the hour-angle of the vernal equinox calculated at epoch. The geographic longitude of the ascending equator crossing was then estimated by turning the earth backward or forward through the orbit angle from the ascending node to the satellite at epoch. This latter quantity was estimated as $\omega + M$, or $360° - (\omega + M)$, for the near-circular orbit of Syncom II. A correction factor to this orbit angle—the ratio of the satellite's period to the earth's sidereal period—was applied for orbits whose period was sufficiently different from the earth's. The nodal longitude at epoch, plus or minus this reduced nodal excursion angle, is the estimated "ascending equator crossing nearest to epoch" reported in Table 1 (see Appendix D for an example of this calculation).

Table 1

Estimated Ascending Equator Crossings Nearest the Epoch of 27 Syncom II Orbits

First Drift Orbits	Time from 20.0 Aug. 1963 (days)	Ascending Equator Crossing (degrees west of 50.0°W)	Second Drift Orbits	Time from 26.0 Nov. 1963 (days)	Ascending Equator Crossing (degrees west of 50.0°W)
1-1	2.12	4.89	2-1	1.86	9.17
1-2	7.11	4.83	2-2	7.84	9.17
1-3	11.09	4.78	2-3	13.83	9.22
1-4	16.08	4.74	2-4	20.81	9.38
1-5	20.07	4.77	2-5	41.75	10.15
1-6	23.06	4.78	2-6	44.74	10.36
1-7	28.05	4.85	2-7	55.71	11.02
1-8	31.04	4.90	2-8	64.69	11.76
1-9	38.02	5.06	2-9	71.67	12.32
1-10	42.01	5.09	2-10	76.66	12.81
1-11	48.99	5.45	2-11	83.64	13.49
1-12	54.97	5.68			
1-13	62.95	6.09			
1-14	70.93	6.60			
1-15	77.91	7.14			
1-16	83.90	7.61			
	≈100.0	First free-drift period ends at an ascending equator crossing of ≈9.15° west of 50.0° West			

Table 2 gives the Goddard-reported semimajor axes for these 27 orbits. Truncating Equations 50 and 53a at their first right-hand terms gives

$$\Delta\lambda \text{ (longitude drift from "synchronism")} \doteq -\left(A_{22} \sin 2\gamma_0\right) \frac{(\Delta t)^2}{2} , \tag{62}$$

$$a_1 \text{ (semimajor axis change from "synchronism")} \doteq A_{22} \frac{\sin 2\gamma_0 \, (\Delta t)}{3\pi} . \tag{63}$$

Let the drift time be given from a certain arbitrary base time by T; let T_0 be the time of "synchronism" from the base time. Let the drift be given from a certain arbitrary geographic longitude by $\underline{\lambda}$ and let $\underline{\lambda}_0$ be the geographic longitude from this base longitude of the "synchronous" configuration. Then

$$\Delta t = T - T_0 ,$$

and

$$\Delta\lambda = \underline{\lambda} - \underline{\lambda}_0 .$$

Table 2

Goddard-Reported Semimajor Axes for 27 Syncom II Orbits

First Drift Orbits	Time from 20.0 Aug. 1963 (days)	Semimajor Axis (42160.0 + data; km)	Second Drift Orbits	Time from 26.0 Nov. 1963 (days)	Semimajor Axis (42160.0 + data; km)
1-1	2.27	4.58	2-1	2.04	5.89
1-2	6.71	4.52	2-2	8.00	7.20
1-3	11.00	6.02	2-3	14.00	7.18
1-4	16.00	6.39	2-4	20.71	8.17
1-5	20.00	6.35	2-5	41.71	8.01
1-6	23.08	6.55	2-6	44.25	9.90
1-7	28.08	6.70	2-7	55.88	11.43
1-8	31.08	7.42	2-8	64.83	11.91
1-9	38.08	7.51	2-9	71.67	12.89
1-10	42.08	8.88	2-10	76.79	13.31
1-11	49.08	9.14	2-11	83.71	14.89
1-12	55.08	9.78			
1-13	63.08	11.51			
1-14	71.00	11.09			
1-15	78.00	12.15			
1-16	84.21	12.51			
	≈100.0	First free drift period ends with a semimajor axis of ≈42174.5 km			

With these changes, Equations 62 and 63 become [noting that $a_1 = (a - a_s)/a_s$]

$$\underline{\lambda} = \underline{\lambda}_0 - \frac{A_{22} \sin 2\gamma_0}{2} T^2 - 2TT_0 + T_0^2 ,$$

or

$$\underline{\lambda} = \left[\underline{\lambda}_0 - \frac{T_0^2 (A_{22} \sin 2\lambda_0)}{2}\right] + T (T_0 A_{22} \sin 2\gamma_0) + T^2 \left(-\frac{A_{22} \sin 2\gamma_0}{2}\right) . \tag{64}$$

(Note that, from Equation 64, $\ddot{\underline{\lambda}} = -A_{22} \sin 2\gamma_0 = \ddot{\gamma}_0$ from Equation 33. This result is valid only for orbits sufficiently close to "synchronous," as discussed previously.)

$$a = a_s + a_s \left(\frac{A_{22} \sin 2\gamma_0}{3\pi}\right)(T - T_0) ,$$

or

$$a = a_s \left(1 - \frac{T_0 A_{22} \sin 2\gamma_0}{3\pi}\right) + T \left(\frac{a_s A_{22} \sin 2\gamma_0}{3\pi}\right) . \tag{65}$$

Equations 64 and 65 may be written with determinable coefficients as

$$\underline{\lambda} = d_0 + d_1 T + d_2 T^2 , \tag{66}$$

$$a = e_0 + e_1 T , \tag{67}$$

where

$$\left.\begin{aligned} d_0 &= \underline{\lambda}_0 - \frac{T_0^2 A_{22} \sin 2\gamma_0}{2} , \\ d_1 &= + A_{22} T_0 \sin 2\gamma_0 , \\ d_2 &= - \frac{A_{22} \sin 2\gamma_0}{2} , \\ e_0 &= a_s \left(1 - \frac{T_0 A_{22} \sin 2\gamma_0}{3\pi}\right) , \\ e_1 &= a_s A_{22} \frac{\sin 2\gamma_0}{3\pi} . \end{aligned}\right\} \tag{68}$$

From Equation 68,

$$T_0 = -d_1/2d_2 \ , \tag{69}$$

$$\lambda_0 = d_0 - \frac{(d_1)^2}{4d_2} \ , \tag{70}$$

$$\ddot{\gamma}_0 = -A_{22} \sin 2\gamma_0 = 2d_2 \ . \tag{71}$$

Alternately, and as an internal check on the theory of the coupling of the drift and orbit expansion,

$$\ddot{\gamma}_0 = -A_{22} \sin 2\gamma_0 = \frac{-3\pi e_1}{a_s} \ ,$$

implying

$$d_2 = 3\pi e_1/2a_s \ . \tag{72}$$

In Equation 72, the units of d_2 must be radians per sidereal day^2, and the units of e_1 must be length per sidereal day so that the equation will be dimensionally correct. The semimajor axis at the "synchronous" configuration is calculated from Equation 67 for $T = T_0$:

$$a_s = e_0 + e_1 T_0 \ . \tag{73}$$

For the first drift period (orbits 1-1 through 1-16), the best estimates (in the "least squares" sense) of the coefficients $(d)_1$ and $(e)_1$, obtained by fitting Equations 66 and 67 to the data in Tables 1 and 2, have been found to be

$$(d_0)_1 = 4.941 \pm 0.018 \text{ degrees},$$

$$(d_1)_1 = -0.0216 \pm 0.0010 \text{ degree/solar day},$$

$$(d_2)_1 = (6.37 \pm 0.11) \times 10^{-4} \text{ degree/solar day}^2$$

$$= (6.33 \pm 0.11) \times 10^{-4} \text{ degree/sid. day}^2,$$

$$(e_0)_1 = 4.35 \pm 0.19 \text{ km},$$

$$(e_1)_1 = 0.0993 \pm 0.0042 \text{ km/solar day}$$

$$= 0.0990 \pm 0.0042 \text{ km/sid. day}.$$

The mean value of the inclination during this period was

$$i_1 = 33.018 \pm 0.005 \text{ degrees.}$$

From Equation 69,

$$(T_0)_1 = \left(16.95 \begin{smallmatrix} + 1.09 \\ - 1.05 \end{smallmatrix}\right) \text{ days from 20.0 August 1963.}$$

From Equation 70,

$$(\lambda_0)_1 = 4.76 \pm 0.03 \text{ degrees west of } 50.0^\circ\text{W long.}$$

From Equation 71,

$$(\ddot{\gamma}_0)_1 = -(1.27 \pm 0.02) \times 10^{-3} \text{ degree/solar day}^2 = -(2.20 \pm 0.04) \times 10^{-5} \text{ rad/sid. day}^2.$$

From Equation 73, and the above value of $(T_0)_1$,

$$(a_s)_1 = 42166.0 \pm 0.2 \text{ km.}$$

For the second drift period (orbits 2-1 through 2-11), the best estimates (in the "least squares" sense) of the coefficients d_2 and e_2, obtained by fitting Equations 66 and 67 to the data in Tables 1 and 2, have been found to be

$$(d_0)_2 = 9.156 \pm 0.017 \text{ degrees,}$$

$$(d_1)_2 = -(0.0030 \pm 0.0010) \text{ degree/solar day,}$$

$$(d_2)_2 = (6.59 \pm 0.11) \times 10^{-4} \text{ degree/solar day}^2,$$

$$= (6.55 \pm 0.11) \times 10^{-4} \text{ degree/sid. day}^2,$$

$$(e_0)_2 = 5.70 \pm 0.42 \text{ km,}$$

$$(e_1)_2 = 0.0994 \pm 0.0080 \text{ km/solar day}$$

$$= 0.0990 \pm 0.0080 \text{ km/sid. day.}$$

The mean value of the inclination during this period was

$$i_2 = 32.851 \pm 0.010 \text{ degrees.}$$

From Equation 69,

$$(T_0)_2 = 2.3 \pm 0.8 \text{ days from 26.0 November 1963.}$$

From Equation 70,

$$(\lambda_0)_2 = 9.15 \pm 0.02 \text{ degrees west of } 50.0^\circ\text{W long.}$$

From Equation 71,

$$(\ddot{\gamma}_0)_2 = -(1.32 \pm 0.02) \times 10^{-3} \text{ degree/solar day}^2 = -(2.29 \pm 0.04) \times 10^{-5} \text{ rad/sid. day}^2.$$

From Equation 73, and the above value of $(T_0)_2$,

$$(a_s)_2 = 42165.9 \pm 0.4 \text{ km.}$$

(See Figure 5 for a graph of this orbit data and reduction for the two drift periods.) Combining the above results of the two free-drift periods, from Equation 60,

$$\frac{(A_{22})_1}{(A_{22})_2} = (42165.9 \pm 0.4/42166.0 \pm 0.2)^2 \frac{\cos^2(33.018 \pm .005) + 1}{\cos^2(32.851 \pm .010) + 1}$$

$$= 0.99845 \pm .00014.$$

The longitude separation between the two drift periods is given by

$$\nabla\lambda = (\lambda_0)_2 - (\lambda_0)_1 = [-(59.15 \pm 0.02)] - [-(54.76 \pm 0.03)] \text{ degrees}$$

$$= -(4.39 \pm 0.05) \text{ degrees geographic longitude.}$$

Thus,

$$2\nabla\lambda = -(8.78 \pm 0.10) \text{ degrees geographic longitude.}$$

Therefore, from Equation 58, the location of the minor equatorial axis with respect to the "synchronous" longitude during the first free-drift period (54.76 ± 0.03 degrees west of Greenwich) is

$$(\gamma_0)_1 = \frac{1}{2} \tan^{-1} \left\{ \frac{\sin[-(8.78 \pm 0.10)]}{\frac{1.32 \pm 0.02}{1.27 \pm 0.02}(0.99845 \pm 0.00014) - \cos[-(8.78 \pm 0.10)]} \right\}$$

$$= \left(54 \begin{smallmatrix} +4 \\ -6 \end{smallmatrix}\right) \text{ degrees east of the minor equatorial axis.}$$

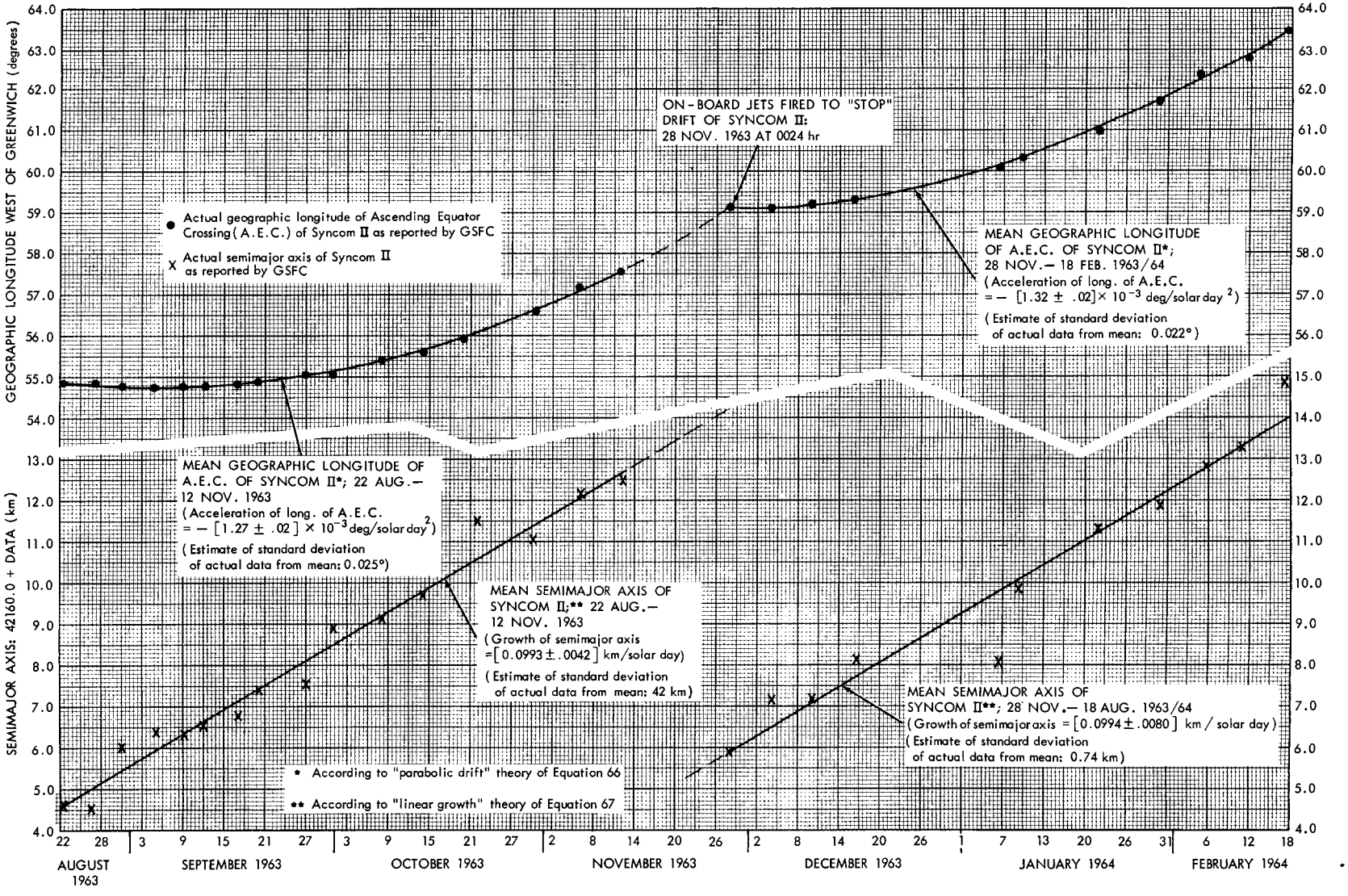

Figure 5—Drift of the ascending equator crossing and growth of the semimajor axis of Syncom II.

From Equation 60b, the best estimate of the location of the major equatorial axis is

$$\lambda_{22} = -55 - \left(54^{+5}_{-6}\right) + 90 = -\left(19^{+5}_{-6}\right) \text{ degrees geographic longitude.} \tag{74}$$

From Equation 59, the best estimate of the triaxial gravity coefficient J_{22} is

$$J_{22} = \frac{-(2.20 \pm 0.04) \times 10^{-5}}{72\pi^2 \sin 2\left(54^{\circ}{}^{+4^{\circ}}_{-6^{\circ}}\right)(6378.2/42166.0 \pm 0.3)^2 \dfrac{\cos^2(33.018 \pm 0.005) + 1}{2}}$$

$$= -\left(1.67^{+0.07}_{-0.03}\right) \times 10^{-6} . \tag{75}$$

The mean equatorial radius, taken as $R_0 = 6378.2$ km, is a compromise for a number of currently used values. It is stated above without error. The likely error in $(a_s)_1$ has been increased arbitrarily by 0.1 km to account for the likely uncertainty in R_0.

The results of the simulated Syncom II trajectories for these drift periods (Appendix C)—with equatorial ellipticity parameters close to Equations 74 and 75 included in the particle program of the simulation—shows that sun, moon, and earth zonal gravity over the 3-month drift periods studied does not substantially affect the simple theory of this reduction.

However, the simulations show small biases in the simple reduction for J_{22} and λ_{22} from Equations 62 and 63 on the basis of an elliptical earth equator only.

The final reduced geodetic parameters adjusted for cumulative sun, moon, and earth zonal gravity effects are:

$$J_{22} = -(1.70 \pm 0.05) \times 10^{-6} \tag{76a}$$

(where J_{22} is adjusted for all but higher order longitude earth-gravity effects), and

$$\lambda_{22} = -(19 \pm 6)^{\circ} \tag{76b}$$

(where λ_{22} is similarly adjusted; see Appendix C). As noted, higher order longitude earth-gravity effects have not been taken account of in these final results.

As can be seen from Figure A1, (the earth's longitude gravity field at the equator according to a recent estimate) the effect of higher order gravity on the results of Equation 76 is not expected to exceed 15 percent on J_{22} and a few degrees on λ_{22}. Figure 6 shows a comparison of the 24-hour altitude longitude gravity field along the equator as derived herein from Syncom II drift over Brazil and three other recent estimates from lower altitude satellite and surface gravity data.

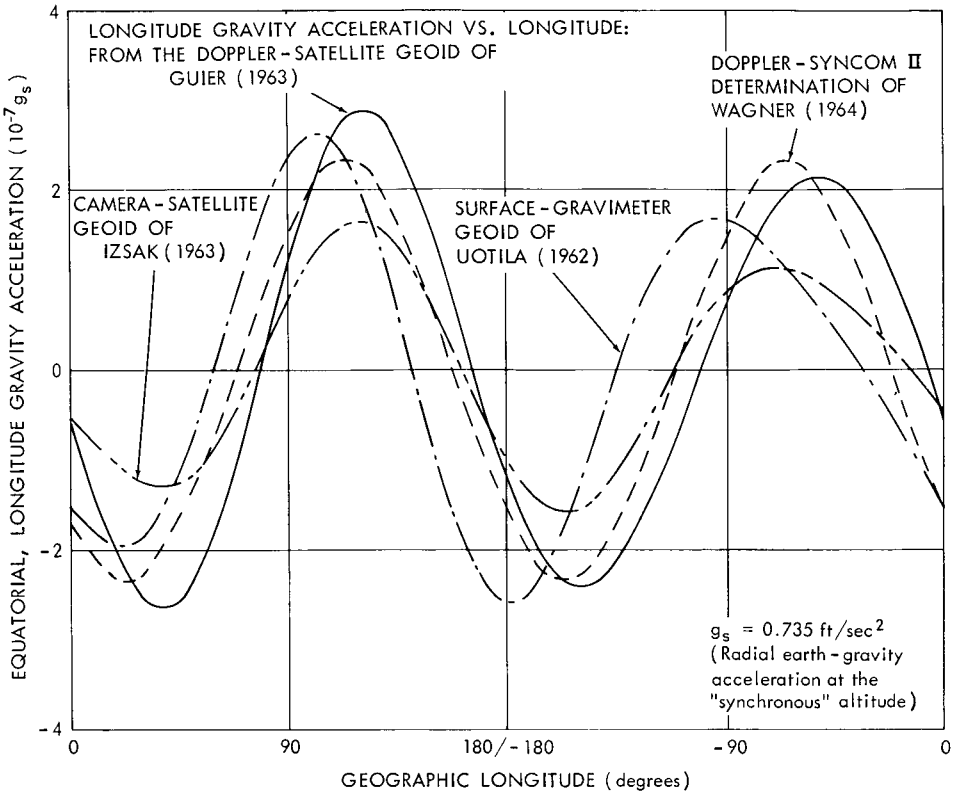

Figure 6—The earth's longitude gravity field at "synchronous altitudes" on the equator, according to recent estimates on different bases (see Table A1).

Using the above estimate of J_{22} from observations on Syncom II drift, the difference between the major and minor equatorial radii of the triaxial geoid is, by Equation 61,

$$a_0 - b_0 = 65 \pm 2 \text{ meters} = 213 \pm 6 \text{ ft.}$$

Comparing the deviation due to earth ellipticity with other higher order earth-gravity deviations (Appendix A*), we note that the above figure implies a maximum deviation from the mean earth sphere, due to the ellipticity of the equator, of

$$\Delta R_0 = 107 \pm 3 \text{ ft.}$$

STATION-KEEPING REQUIREMENTS FOR EQUATORIAL 24-HOUR SATELLITES

Following the calculation first made by Fleig,† maximum station-keeping requirements for a synchronous equatorial satellite in a purely triaxial earth field occur at a longitude 45 degrees

*Also, Wagner, *op. cit.* (See footnote, p. 7).

†Fleig, A., "Effect of Nonsphericity of Earth's Gravitational Potential on an Equatorial Synchronous Satellite," NASA Goddard Space Flight Center, Guidance and Control Section (Code 622) Report 43, June 15, 1962.

from the major axis of the elliptical equator. The triaxial longitude perturbation force which must be continually counteracted by on-board propulsion devices to achieve perfect station keeping is given in Appendix A (Equation A4) as

$$(F_\lambda)_{22} = \frac{\mu_E}{(a_s)^2}\left(\frac{R_0}{a_s}\right)^2 \left[6J_{22} \sin 2(\lambda - \lambda_{22})\right] \quad . \tag{77}$$

The maximum perturbation force occurs at longitudes where $\lambda - \lambda_{22} = \pm 45, \pm 135$ degrees; or, for the reported adjusted value, $\lambda_{22} = -19$ degrees; maximum perturbation forces occur at

$$\lambda = -64, -154, 116, 26 \text{ degrees} . \tag{78}$$

For the reported adjusted value; $J_{22} = -(1.7) \times 10^{-6}$, with

$$\mu_E/(a_s)^2 = 0.735 \text{ ft/sec}^2 . (R_0/a_s)^2 = 0.0229 ,$$

the maximum yearly impulse per unit mass, or velocity requirement for perfect station keeping (at these longitudes), is:

$$\begin{aligned}(F_\lambda)_{22,max} \times T(1 \text{ year}) = \Delta V_{T,max} &= 0.735 \times 0.0229 \times 86,400 \times 365 \times 6 \times 1.70 \times 10^{-6} \\ &= 5.36 \text{ ft/sec/yr} .\end{aligned} \tag{79}$$

The result in Equation 79 is strictly true only for a triaxial earth field. As Reference 4 shows, and the combined geoid of Kaula (1964) confirms, the absolute maximum longitude perturbation (at 24-hour altitudes) in a full earth field may increase by as much as 15 percent over that in the simple triaxial field. According to the combined geoid of Kaula (1964), this absolute maximum longitude perturbation occurs over Indonesia (see Figure A1, Appendix A).

For synchronous satellites to be kept permanently in this quadrant may require, conservatively,

$$\Delta V_{T,\text{abs max}} \doteq 6.17 \text{ ft/sec/yr} . \tag{80}$$

However, this latter result may not be conservative enough if there is an additional bias in the reported value of J_{22} (in Equation 76) due to the neglect, in that reduction, of these same higher order effects. A study of Kaula's geoid of Figure A1, Appendix A, certainly indicates that such a bias would be present for a J_{22}-only reduction from the full field effects at the two longitudes -54.8 and -59.2 degrees. An investigation is underway by the author of these probable higher order effects on the reported Syncom II geodetic reductions from drift over Brazil (Equation 76).

DISCUSSION OF RESULTS

Some discussion is in order on the validity of the reported geodetic parameters (Equation 76). These adjusted parameters, without accounting for higher order earth-gravity

effects, show a somewhat stronger and west-shifted equatorial ellipticity than the most recent satellite geoids (see Table A1, Appendix A). Around the equator, the reported Syncom II determination yields a longitude gravity field at 24-hour altitudes in reasonable agreement with recent satellite and surface gravimeter determinations (see Figure 6). The basic assumption behind the reported Syncom II determination is that during the analyzed drift periods the satellite moved free of all external influences except sun, moon, and earth gravity.

It seems very unlikely that other small influences on Syncom II motion, such as (1) micrometeorite collisions, (2) possible leaking gas from the satellite, (3) solar radiation and solar wind pressure, (4) magnetic field interactions, and (5) planetary gravity, could have had appreciable selective influence on the observed accelerated drift of the satellite. The fact is that the simulated Syncom II drifts (Appendix C) in a sun, moon, and earth-gravity field only reproduce the observed drifts in all particulars to a degree which seems to preclude other influences except small random ones.

From injection to mid-August 1963, there appeared to be some question as to possible leaking of gas on board Syncom II. Monitored gas pressure levels in some of the propellant tanks declined erratically between correction maneuvers in this period. However, levels were reasonably constant in the analyzed long free-drift periods. The evidence of erratic and declining gas pressure levels on board Syncom II is thought to be due, at least in part, to pressure transducer calibration errors.

Sun, moon, and zonal earth-gravity influences on Syncom II's long-term drift acceleration, as well as model errors made in the assumptions of orbit circularity and unchanging inclination, have been accounted for in the simulated drift reductions. As yet, only two sustained longitude samples of the earth's gravity field have been taken by a 24-hour satellite. It is noted from the evidence of Figure A1 (Appendix A) and Reference 4* that the "true value" of the magnitude of equatorial ellipticity, when all higher order earth-gravity effects are accounted for, may be as much as 15 percent higher than that reported herein. With the next few samplings at reasonably separated longitudes, a considerable refinement in the estimate of equatorial ellipticity (as affected by higher order gravity) should be possible. Along with this refinement should come an order-of-magnitude estimate of third- (and higher) order longitude earth gravity. Much geodetic information remains to be revealed by closely following the drift of Syncom II and other 24-hour satellites soon to be launched by NASA.

CONCLUSIONS

From this investigation into longitude-gravity-caused Syncom II drift, the following conclusions are made:

1. Longitude-dependent earth gravity exists and must be reckoned with in the long-term operation of 24-hour satellites.

*Also: Private communication from W. M. Kaula, 1964, "Theory of Satellite Geodesy," (unpublished text for a course at the Institute of Geophysics and Planetary Physics, UCLA, Los Angeles, Calif.)

2. As far as 24-hour satellites are concerned, the earth can be assumed to be only a triaxial ellipsoid with the following measures of equatorial ellipticity:

$$(a) \qquad J_{22} = -(1.70 \pm 0.05) \times 10^{-6} \ ,$$

corresponding to a 65 ± 2 meter difference between major and minor equatorial radii;

$$(b) \qquad \lambda_{22} = -(19 \pm 6)^{\circ} \ ,$$

locating the geographic longitude of the major equatorial axis.

3. Higher order earth-gravity effects appear to distort the simple triaxial field at 24-hour altitudes, by about 10 to 15 percent, at most, around the equator. A few of these effects of the third- and fourth-order should be well discriminated by long-term observations of future 24-hour satellites.

4. With negligible higher order earth effects assumed, the maximum longitude gravity station-keeping requirements for the 24-hour satellite are 5.36 ft/sec/yr.

ACKNOWLEDGMENT

The author appreciates the generous cooperation of Dr. David Mott, New Mexico State University, in critically reviewing the ideas behind this work both before and after the preparation of this paper.

(Manuscript received: September 24, 1964)

REFERENCES

1. Blitzer, L., Boughton, E. M., Kang, G., and Page, R. M., "Effect of Ellipticity of the Equator On 24-Hour Nearly Circular Satellite Orbits," *J. Geophys. Res.* 67:329-335, 1962.

2. Heiskanen, W. A., and Meinesz, F. A., "The Earth and Its Gravity Field," New York: McGraw-Hill, 1958.

3. Izsak, I. G., "Tesseral Harmonics In The Geopotential," *Nature* 137-139, July 13, 1963.

4. Wagner, C. A., "The Drift of a 24-Hour Equatorial Satellite Due To An Earth Gravity Field Through 4th Order," NASA TN-D-2103, February 1964.

5. Allan, R. R., "Perturbations of a Geostationary Satellite by the Longitude Dependent Terms in the Earth's Gravitational Field," in *Planetary Space Sci.*, vol. 11, pp. 1325-1334, 1963.

6. Musen, P., "On The Motion Of A 24-Hour Satellite," *J. Geophys. Res.* 67(3):1123-1132, 1962.

7. Thomson, W. T., "Introduction To Space Dynamics," p. 72, New York: Wiley, 1961.

8. Kozai, Y., "The Earth's Gravitational Potential Derived from Motions of Three Satellites," *Astronom. J.* 66:8-10, 1961.

9. O'Keefe, J. A., Eckels, A., and Squires, R. K., "The Gravitational Field of the Earth," *Astronom. J.* 64:245-253, 1959.

10. Salvadori, M. G., and Schwarz, R. J., "Differential Equations In Engineering Problems," Chap. 9, Englewood Cliffs, N. J.: Prentice-Hall, 1954.

11. Jahnke, E., and Emde, F., "Tables of Functions," 1945 ed., Chap. V, New York: Dover, 1945.

Appendix A

Earth-Gravity Potential and Force Field Used in this Report: Comparison with Previous Investigations

The gravity potential used as the basis for the data reduction in this study is the exterior potential of the earth derived* for geocentric spherical coordinates referenced to the earth's spin axis and its center of mass. The infinite series of spherical harmonics is truncated after J_{44}. The nontesseral harmonic constants J_{20}, J_{30}, and J_{40} are derived from Reference 8.

The earth radius R_0 used in this study is

$$R_0 = 6378.388 \text{ km}.$$

The earth's gaussian-gravity constant used is

$$\mu_E = 3.9862677 \times 10^5 \text{ km}^3/\text{sec}^2.$$

Neither of these values, taken from Reference 9, nor the "zonal geoid" of Reference 8 is felt to be the most accurate known to date. They are the values used by the GSFC Tracking and Data Systems Directorate to calculate the orbit elements of Syncom II from radar and Minitrack observations. They were chosen to insure consistency between the data of this study and these published orbits, inasmuch as the "triaxial" reduction for which this study has been undertaken is not significantly affected by the probable errors in these values. The second-order tesseral harmonic constants used in the simulation studies were

$$J_{22} = -1.68 \times 10^{-6},$$

$$\lambda_{22} = -18 \text{ degrees}.$$

These are the values shown on the "tesseral geoid" below (for the J_{22} harmonic). At a later point in the analysis, the slightly different values reported in the abstract were estimated. The most accurate "zonal geoid" is probably that of Kozai (see Reference 4), with the following earth constants:

$$R_0 = 6378.2 \text{ km},$$

$$J_{20} = 1082.48 \times 10^{-6}, \quad J_{30} = -2.56 \times 10^{-6}, \quad J_{40} = -1.84 \times 10^{-6},$$

$$\mu_E = 3.98603 \times 10^5 \text{ km}^3/\text{sec}^2.$$

The earth's gravity potential (to fourth order, probably sufficient to account for all significant longitude perturbations on a 24-hour satellite) is given by Equation A1, which may be illustrated as follows (following Reference 4, Appendix B):

*Wagner, *op. cit.* (See footnote, p. 7.)

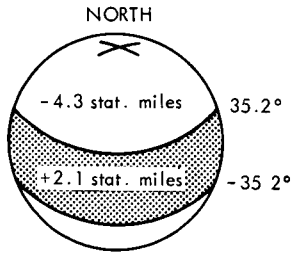

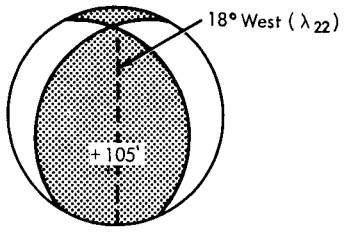

$$V_E = \frac{\mu_E}{r}\left[1 - \frac{J_{20} R_0^2}{2r^2}\left(3\sin^2\phi - 1\right) - 3J_{22}\frac{R_0^2}{r^2}\cos^2\phi\cos 2\left(\lambda - \lambda_{22}\right)\right.$$

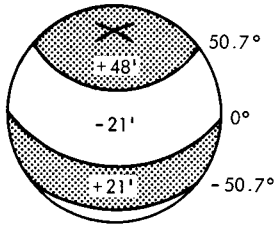

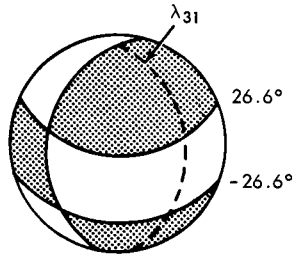

$$\left. - \frac{J_{30} R_0^3}{2r^3}\left(5\sin^3\phi - 3\sin\phi\right) - \frac{J_{31} R_0^3}{2r^3}\cos\phi\left(15\sin^2\phi - 3\right)\cos\left(\lambda - \lambda_{31}\right)\right.$$

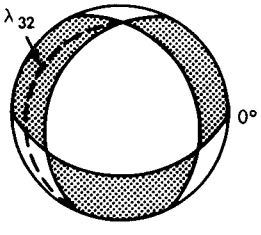

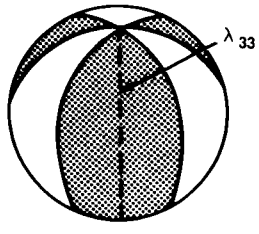

$$\left. - 15J_{32}\frac{R_0^3}{r^3}\cos^2\phi\sin\phi\cos 2\left(\lambda - \lambda_{32}\right) - 15J_{33}\frac{R_0^3}{r^3}\cos^3\phi\cos 3\left(\lambda - \lambda_{33}\right)\right.$$

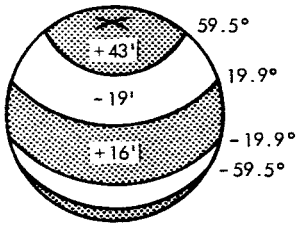

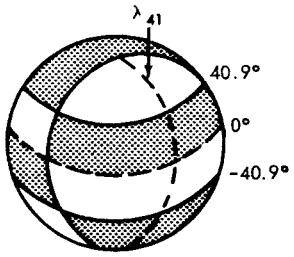

$$-\frac{J_{40}R_0^4}{8r^4}\left(35\sin^4\phi - 30\sin^2\phi + 3\right) - \frac{J_{41}R_0^4}{8r^4}\left(140\sin^3\phi - 60\sin\phi\right)\cos\phi\cos\left(\lambda - \lambda_{41}\right)$$

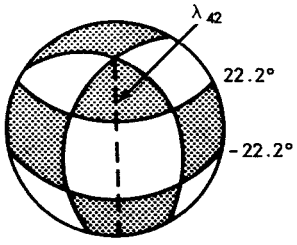

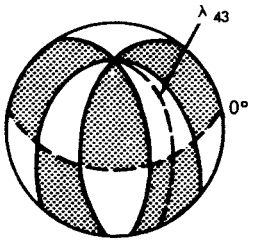

$$-\frac{J_{42}R_0^4}{8r^4}\left(420\sin^2\phi - 60\right)\cos^2\phi\cos 2\left(\lambda - \lambda_{42}\right) - \frac{J_{43}R_0^4}{8r^4}\,840\sin\phi\cos^3\phi\cos 3\left(\lambda - \lambda_{43}\right)$$

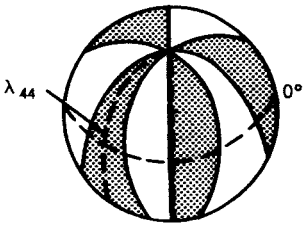

$$-\frac{J_{44}R_0^4}{8r^4}\,840\cos^4\phi\cos 4\left(\lambda - \lambda_{44}\right)\Bigg] \quad . \tag{A1}$$

The earth-gravity field (per unit test mass), whose potential is Equation A1, is given as the gradient of A1, or

$$\bar{F} = \hat{r}F_r + \hat{\lambda}F_\lambda + \hat{\phi}F_\phi = \nabla V_E = \hat{r}\frac{\partial V_E}{\partial r} + \frac{\hat{\lambda}}{r\cos\phi}\frac{\partial V_E}{\partial \lambda} + \frac{\hat{\phi}}{r}\frac{\partial V_E}{\partial \phi} \quad ; \tag{A2}$$

or

$$\begin{aligned} F_r = \frac{\mu_E}{r^2}\Big\{ & -1 + (R_0/r)^2\Big[3/2 J_{20}\left(3\sin^2\phi - 1\right) + 9J_{22}\cos^2\phi\cos 2\left(\lambda - \lambda_{22}\right) \\ & + 2(R_0/r)\, J_{30}\left(5\sin^2\phi - 3\right)(\sin\phi) + 6(R_0/r)\, J_{31}\left(5\sin^2\phi - 1\right)\cos\phi\cos\left(\lambda - \lambda_{31}\right) \\ & + 60(R_0/r)\, J_{32}\cos^2\phi\sin\phi\cos 2\left(\lambda - \lambda_{32}\right) + 60(R_0/r)\, J_{33}\cos^3\phi\cos 3\left(\lambda - \lambda_{33}\right) \\ & + 5/8(R_0/r)^2 J_{40}\left(35\sin^4\phi - 30\sin^2\phi + 3\right) \\ & + 25/2(R_0/r)^2 J_{41}\left(7\sin^2\phi - 3\right)\cos\phi\sin\phi\cos\left(\lambda - \lambda_{41}\right) \\ & + 75/2(R_0/r)^2 J_{42}\left(7\sin^2\phi - 1\right)\cos^2\phi\cos 2\left(\lambda - \lambda_{42}\right) \\ & + 525(R_0/r)^2 J_{43}\cos^3\phi\sin\phi\cos 3\left(\lambda - \lambda_{43}\right) + 525(R_0/r)^2 J_{44}\cos^4\phi\cos 4\left(\lambda - \lambda_{44}\right)\Big]\Big\} , \end{aligned} \tag{A3}$$

$$\begin{aligned} F_\lambda = \frac{\mu_E}{r^2}(R_0/r)^2\Big\{ & 6J_{22}\cos\phi\sin 2\left(\lambda - \lambda_{22}\right) + 3/2(R_0/r)\, J_{31}\left(5\sin^2\phi - 1\right)\sin\left(\lambda - \lambda_{31}\right) \\ & + 30(R_0/r)\, J_{32}\cos\phi\sin\phi\sin 2\left(\lambda - \lambda_{32}\right) + 45(R_0/r)\, J_{33}\cos^2\phi\sin 3\left(\lambda - \lambda_{33}\right) \\ & + 5/2(R_0/r)^2 J_{41}\left(7\sin^2\phi - 3\right)\sin\phi\sin\left(\lambda - \lambda_{41}\right) + 15(R_0/r)^2 J_{42}\left(7\sin^2\phi - 1\right)\cos\phi\sin 2\left(\lambda - \lambda_{42}\right) \\ & + 315(R_0/r)^2 J_{43}\cos^2\phi\sin\phi\sin 3\left(\lambda - \lambda_{43}\right) \\ & + 420(R_0/r)^2 J_{44}\cos^3\phi\sin 4\left(\lambda - \lambda_{44}\right)\Big\} , \end{aligned} \tag{A4}$$

$$F_\phi = \frac{\mu_E}{r^2}(R_0/r)^2\Big\{-3J_{20}\sin\phi\cos\phi + 6J_{22}\cos\phi\sin\phi\cos 2(\lambda-\lambda_{22})$$

$$-3/2(R_0/r)\,J_{30}\,(5\sin^2\phi-1)\cos\phi + 3/2(R_0/r)\,J_{31}\,(15\sin^2\phi-11)\sin\phi\cos(\lambda-\lambda_{31})$$

$$+15(R_0/r)\,J_{32}\,(3\sin^2\phi-1)\cos\phi\cos 2(\lambda-\lambda_{32})$$

$$+45(R_0/r)\,J_{33}\cos^2\phi\sin\phi\cos 3(\lambda-\lambda_{33}) - 5/2(R_0/r)^2\,J_{40}\,(7\sin^2\phi-3)\sin\phi\cos\phi$$

$$+5/2(R_0/r)^2\,J_{41}\,(28\sin^4\phi-27\sin^2\phi+3)\cos(\lambda-\lambda_{41})$$

$$+30(R_0/r)^2\,J_{42}\,(7\sin^2\phi-4)\cos\phi\sin\phi\cos 2(\lambda-\lambda_{42})$$

$$+105(R_0/r)^2\,J_{43}\,(4\sin^2\phi-1)\cos^2\phi\cos 3(\lambda-\lambda_{43})$$

$$+420(R_0/r)^2\,J_{44}\cos^3\phi\sin\phi\cos 4(\lambda-\lambda_{44})\Big\} \qquad \text{(A5)}$$

The actual sea-level surface of the earth is to be conceptualized through Equation A1 as a sphere of radius 6378 km, around which are superimposed the sum of the separate spherical harmonic deviations illustrated. To these static gravity deviations, of course, must be added a centrifugal earth-rotation potential at the earth's surface, to get the true sea-level surface.*

Table A1 gives tesseral coefficients for this earth-gravity field form as reported by geodesists from 1859 to 1964. Figure A1 presents the longitude gravity field at the altitude of the 24-hour satellite, around the equator, according to the geoid of Kaula-Combined (1964). Figures A2 through A8 give the earth surface contours of seven recent geoids whose individual tesseral coefficients are listed in Table A1.

*Wagner, *op. cit.* (See footnote, p. 7.)

Table A1

TESSERAL COEFFICIENTS IN THE EARTH'S GRAVITY POTENTIAL $\left\{ V_E = \frac{\mu}{r} \sum_{n=2}^{\infty} \sum_{m=0}^{n} \left[1 - (R_0/r)^n P_n^m (\sin \phi) J_{nm} \cos m (\lambda - \lambda_{nm}) \right] \right\}$ AS REPORTED 1859-1964*

TESSERAL GEOID†	J_{22}	λ_{22}	J_{31}	λ_{31}	J_{32}	λ_{32}	J_{33}	λ_{33}	J_{41}	λ_{41}	J_{42}	λ_{42}	J_{43}	λ_{43}	J_{44}	λ_{44}
(1) Wagner (1964)[A]	-1.7×10^{-6}	-19.0°														
(2) Kaula-Combined (1964)[E]	-1.51	-15.5	-1.51×10^{-6}	0.0°	-0.102×10^{-6}	0.0°	-0.149×10^{-6}	22.8°	-0.465×10^{-6}	-136.0°	-0.163×10^{-6}	37.0°	-0.061×10^{-6}	- 1.9°	-0.0053×10^{-6}	35.8°
(3) Izsak (1964)[B]	-1.00	-17.0	-0.934	-15.5	-0.116	19.0	-0.173	38.0	-0.949	-146.0	-0.074	47.5	-0.024	- 3.9	-0.0206	25.3
(4) Kaula (1964)[B]	-1.77	-18.2	-2.12	- 5.4	-0.379	10.5	-0.105	23.1	-0.263	-239.0	-0.117	42.3	-0.0473	15.0	-0.0104	14.5
(5) Anderle and Oesterwinter (1963)[A]	-2.09	-14.1							-0.773	-140.6	-0.287	34.7	-0.163	- 4.3		
(6) Guier (1963)[A]	-1.80	-10.4	-1.77	6.3	-0.286	- 2.6	-0.204	24.1	-0.73	-141.0	-0.273	38.6	-0.0791	- 0.7	-0.0102	35.0
(7) Kaula (Sept. 1963)[B]	-1.51	-18.1	-1.65	5.3	-0.144	46.4	-0.145	15.8	-0.471	-228.0	-0.078	44.2	-0.0265	22.6	-0.0038	23.3
(8) Izsak (July 1963)[B]	-1.05	-11.2	-1.1	3.2	-0.20	-21.8	-0.14	20.0	-0.43	-132.1	-0.13	37.0	-0.026	11.5	-0.019	14.8
(9) Kaula (May 1963)[B]	-1.4	-21.5	-1.6	- 1.9	-0.15	35.8	-0.156	18.5	-0.53	-233.7	-0.12	44.5	-0.019	10.7	-0.0038	23.3
(10) Cohen (May 1963)[A]	-2.08	-14.1							-0.775	-159.0	-0.288	34.6	-0.162	- 4.3		
(11) Kaula (Jan. 1963)[B]	-1.62	-21.4	-1.81	- 3.57	-0.145	6.6	-0.112	37.6	-0.479	-245.5	-0.072	47.7	-0.0988	5.9	-0.0132	28.4
(12) Uotila (1962)[C]	-1.52	-36.5	-0.685	-81.0	-0.409	- 5.2	-0.398	19.5	-0.238	-127.0	-0.211	14.6	-0.082	- 9.3	-0.0142	- 2.6
(13) Kozai (Oct. 1962)[B]	-1.2	-26.4	-1.9	4.6	-0.14	-16.8	-0.10	42.6	-0.52	-122.5	-0.062	65.2	-0.035	0.5	-0.031	14.9
(14) Newton (April 1962)[A]	-2.15	-10.9							-2.53	-189.1						
(15) Newton (Jan. 1962)[A]	-4.16	-11.0														
(16) Kozai (June 1961)[B]	-2.32	-37.5	-3.21	22.0	-0.41	31.0	-1.91	51.3	-0.262	-196.5	-0.168	54.0	-0.044	-13.0	-0.054	50.3
(17) Kaula (June 1961)[E]	-0.55	-13.3	-1.19	20.6	-0.33	- 0.9	-0.21	22.6	-0.617	-166.0	-0.14	21.1	-0.031	- 0.5	-0.008	26.4
(18) Izsak (Jan. 1961)[B]	-5.35	-33.2														
(19) Kaula (1961)[C]	-1.68	-38.5							-1.15	- 13.0						
(20) Kaula (1959)[C]	-0.62	-20.9	-0.98	55.4	-0.11	13.3	-0.19	14.3	-0.46	-132.3	-0.081	48.6	-0.01	-30.0	-0.02	22.5
(21) Jeffreys (1959)[C]	-4.17	0.0														
(22) Uotila (1957)[C]	-3.5	- 6.0														
(23) Zhongolovitch (1957)[C]	-5.95	- 7.7	-2.21	-25.7	-0.628	-26.4	-0.54	13.0	-0.78	-149.1	-0.080	45.0	-0.051	- 3.8	-0.0224	15.9
(24) Subbotin (1949)[C]	-5.5															
(25) Lambert (1945)[C]	-9.2	-25.0														
(26) Niskanen (1945)[C]	-7.67	- 4.0														
(27) Krassowski (1942)[D]	-5.6	15.0														
(28) Jeffreys (1942)[C]	-4.1	0.0	-2.1	0.0	-0.66	0.0	-0.24	33.3								
(29) Heiskanen (1938)[C]	-9.2	-25.0														
(30) Hirvonen (1934)[C]	-3.6	-19.0														
(31) Heiskanen (1929)[C]	-4.3	38.0														
(32) Heiskanen (1928)[C]	-6.34	0.0														
(33) Heiskanen (1924)[C]	-9.0	18.0														
(34) Berroth (1916)[C]	-3.9	-10.0														
(35) Helmert (1915)[C]	-6.0	-17.0														
(36) Hill (1884)[D]	-32.9	17.0														
(37) Clarke (1878)[D]	-12.1	- 8.0														
(38) Clarke (1866)[D]	-50.9	15.0														
(39) Clarke (1860)[D]	-42.3	14.0														
(40) Schubert (1859)[D]	-18.8	41.0														

*(r is the radial distance of the field point to the center of mass of the earth, μ the earth's Gaussian gravity constant $\doteq 3.9860 \times 10^{20} \text{cm}^3/\text{sec}^2$, R_0 the mean equatorial radius of the earth $\doteq$ 6378.2 km; ϕ is the geocentric latitude of the field point, λ the geographic longitude of the field point; $J_{21} = 0$, since the polar axis is very nearly a principal axis of inertia for the earth. $P_n^m(\sin \phi) = \cos^m \phi \sum_{t=0}^{K} T_{nmt} \sin^{n-m-2t} \phi$, where K is the integer part of $(n - m)/2$ and $T_{nmt} = (-1)^t (2n - 2t)! / 2^n t! (n - t)! (n - m - 2t)!$ (see footnote, p. 32); the tesseral coefficients are those for which $(m \neq 0)$.

The J_{nm}'s and λ_{nm}'s in this table, except in one or two instances, have been converted from the original authors' set of gravity coefficients. The blanks indicate the author did not consider that particular harmonic in fitting an earth potential to the observed data. In one or two instances (noted below) the author reported tesseral coefficients to higher order than the fourth.

†The second page of Table A1 consists of a list of references and comments for geoids (1)-(40). The superscript letters A-E in this column indicate the type of geoid as given below:

[A]Satellite-Doppler geoid

[B]Satellite-camera geoid

[C]Surface-gravimetric geoid

[D]Astrogeodetic geoid

[E]Combined astrogeodetic, gravimetric, and satellite geoid

Table A1 (Continued)

GEOID	REFERENCES	COMMENTS
(1)	"Determination of the Triaxiality of the Earth from Observations on the Drift of the Syncom II Satellite," NASA Goddard Space Flight Document X-621-64-90, April 1964.	Uses 7 months of Doppler data during longitude drift over Brazil.
(2)	Private communication from W. M. Kaula, July 1964.	A weighted average of geoids (3),(4),(5),(6),(12),(13), and (17).
(3),(4)	Private communication from W. M. Kaula, July 1964.	Geoid (3) is a revision of (8) with new data; (4) is a revision of (7) with new data.
(5)	Private communication from W. M. Kaula, July 1964.	Appears to be a revision of geoid (10).
(6),(10),(14)	In: "Non-Zonal Harmonic Coefficients of the Geopotential from Satellite Doppler Data," W. H. Guier and R. R. Newton, Johns Hopkins Univ. APL-TG-520, Nov. 1963.	
(7)	"Improved Geodetic Results from Camera Observations of Satellites," J. Geophys. Res. 68(18), Sept. 1963.	Uses five satellites, of medium and high inclination.
(8)	"Tesseral Harmonics in the Geopotential," Nature, pp. 137-139 July 13, 1963.	Uses five satellites, of medium and high inclination.
(9)	Private communication from W. M. Kaula, May 1963.	Uses three satellites of medium inclination.
(11)	"Tesseral Harmonics of the Gravitational Field and Datum Shifts Derived from Camera Observations of Satellites," J. Geophys. Res. 68(2), Jan. 15, 1963.	Uses three satellites of medium inclination.
(12)	Private Communication from W. M. Kaula, July 1964.	
(13)	Private communication from Y. Kozai, Oct. 1962.	
(14)	Private communication from Newton, April 1962.	
(15)	"Ellipticity of the Earth's Equator Deduced from the Motion of Transit 4A," J. Geophys. Res. 67(1), Jan. 1962.	
(16)	"Tesseral Harmonics of the Gravitational Potential of the Earth as Derived from Satellite Motions," Astronom. J. 66(7), Sept. 1961.	Uses three satellites of medium inclination.
(17)	"A Geoid and World Geodetic System Based on a Combination of Gravimetric, Astrogeodetic, and Satellite Data," J. Geophys. Res. 66(6):1807, 1961.	Considers tesserals to eighth order.
(18)	From: Astronom. J. 66(5):226-229, June 1961.	Uses two satellites of medium inclination.
(19)	In: Space Research II, pp. 360-372; H. C. Van De Hulst, Ed: North Holland Publishing Co., Amsterdam.	
(20)	In: J. Geophys. Res. 64:2401, 1959.	
(21)	"The Earth," Cambridge Univ. Press: N.Y., 4th edition, chapt. IV, V.	
(22),(26),(32),(33),(35)	"The Earth and its Gravity Field," McGraw-Hill: N.Y., p. 79, 1958.	
(23)	In: Bull. Inst. Theoret. Astron. 6:505.	
(24)	"Course in Celestial Mechanics III," Gostchizdat: Moscow, p. 278, 1958.	
(27)	In: "Passive Dynamics in Space Flight," Bureau of Naval Weapons paper by J. D. Nicolaides and M. M. Macomber, 1962.	
(28),(27)	In: Monthly Notices Royal Astronom. Soc. Geophys. Suppl., 5(55), 1942.	
(27),(25),(29)-(31),(34),(36)-(40)	In: "Is the Earth a Triaxial Ellipsoid?" W. A. Heiskanen, J. Geophys. Res. 67(1), Jan. 1962.	

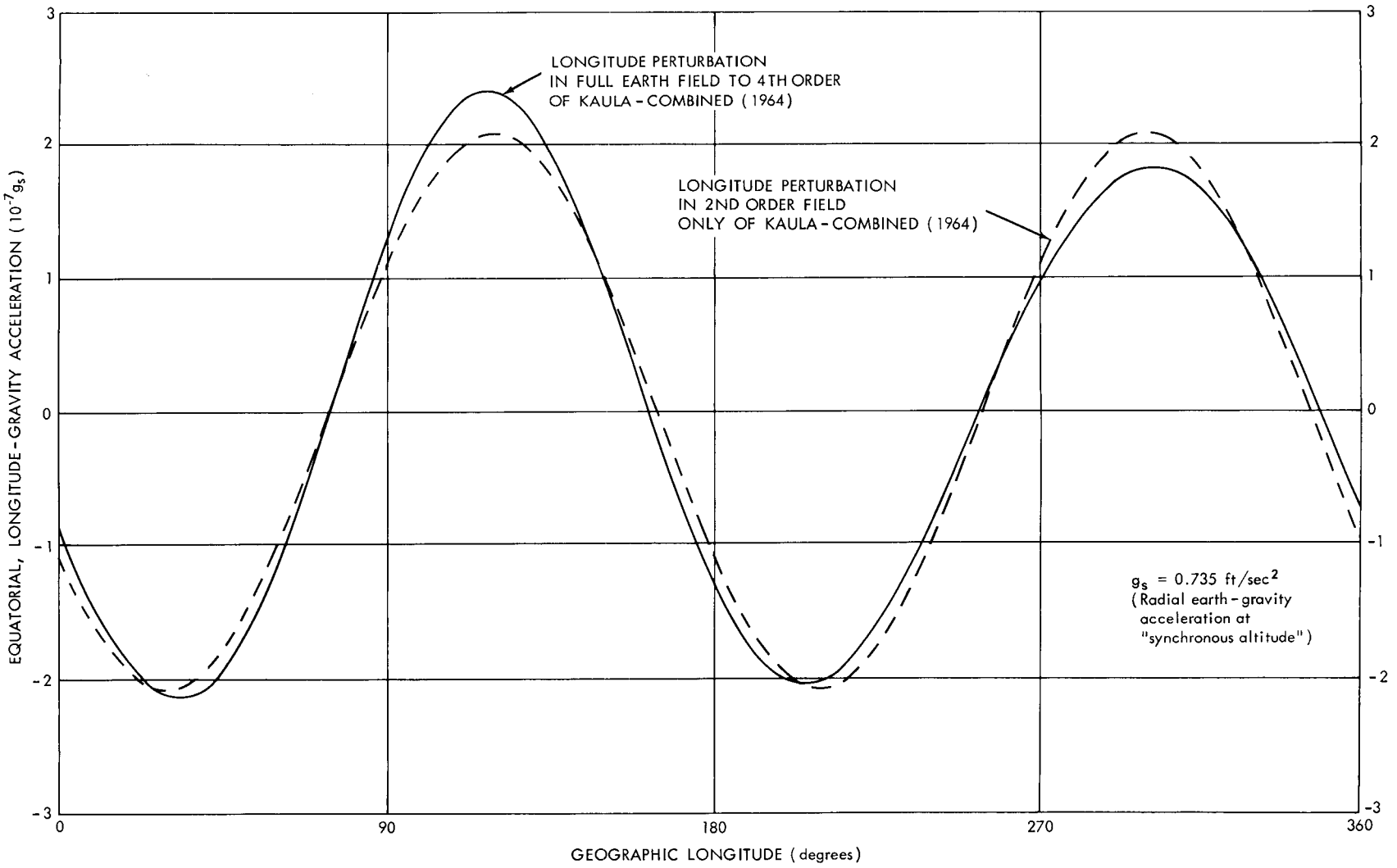

Figure A1—The earth's longitude gravity field on the equator at the synchronous altitude, according to geoid (4), Table A1.

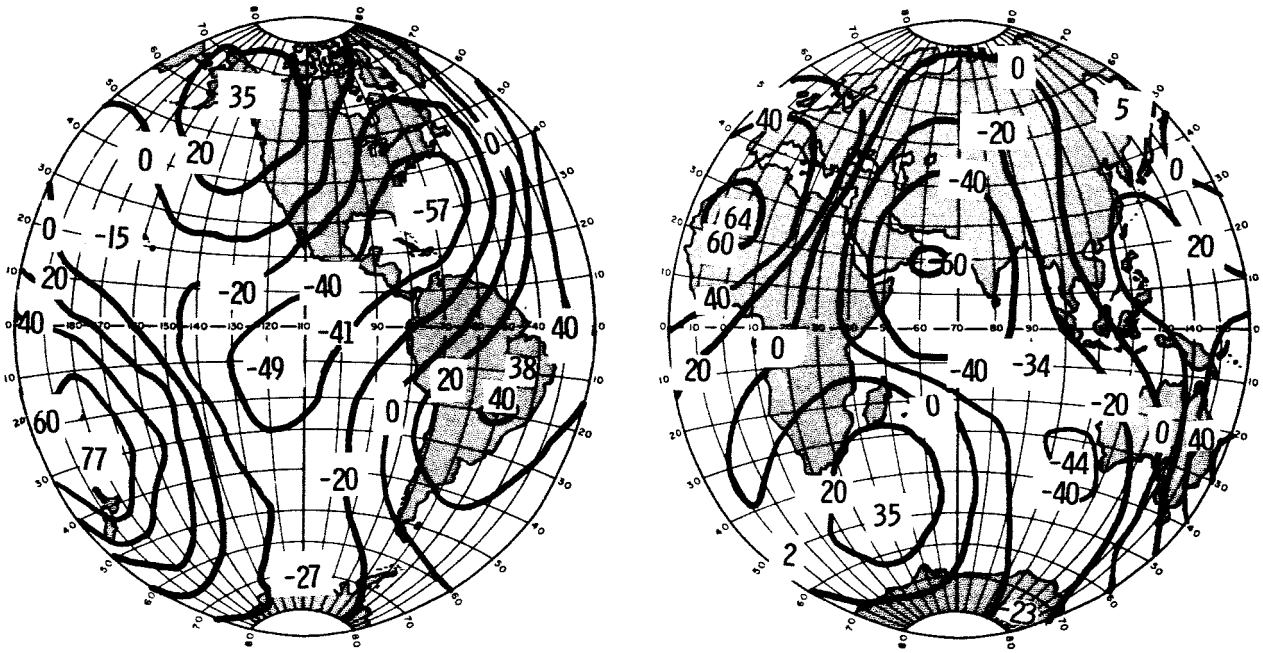

Figure A2—Satellite-Doppler geoid [(5), Table A1]. Note: In Figures A2-A8, geoid height (in meters) refers to an ellipsoid of flattening 1/298.24; after Kaula, geoid (17).*

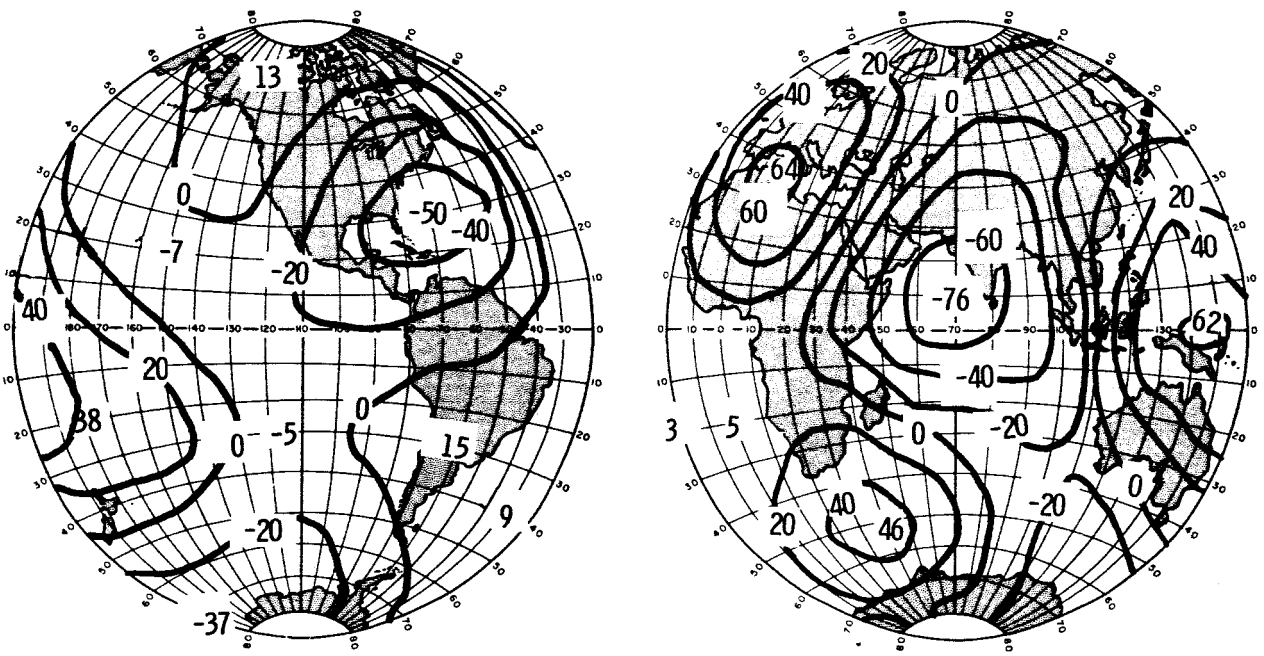

Figure A3—Satellite-Doppler geoid [(6), Table A1].

*These geoid representations were supplied by W. M. Kaula in a communication to the author, October 1964.

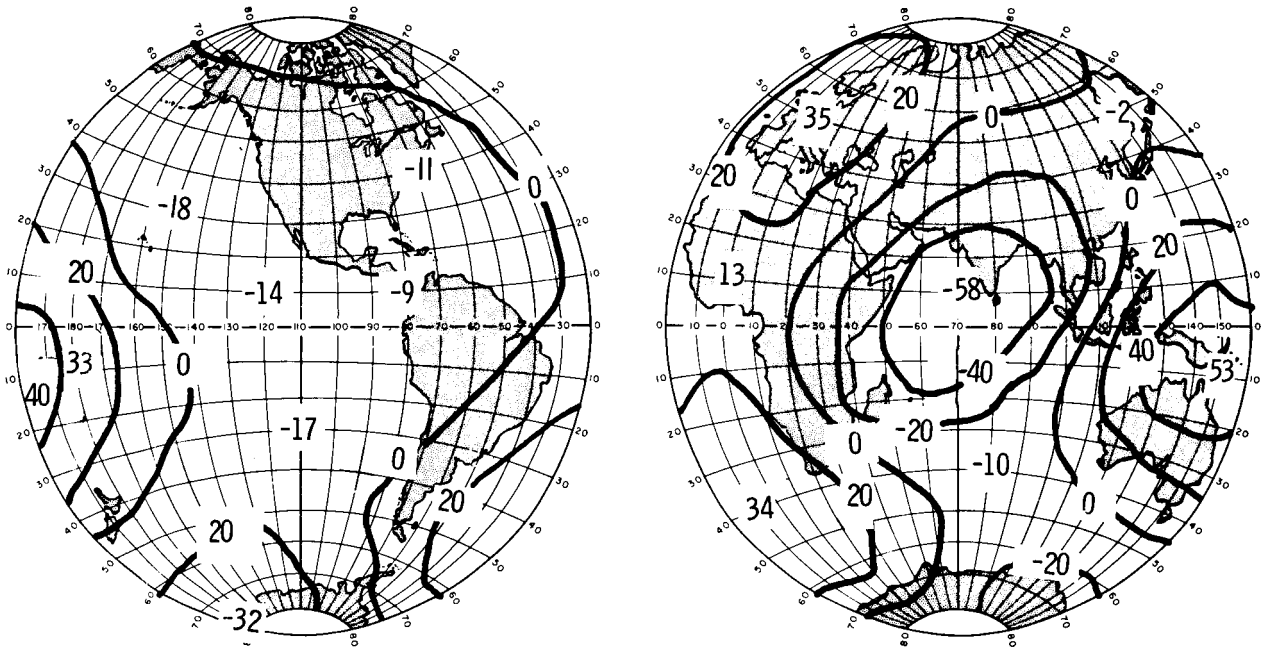

Figure A4—Satellite-camera geoid [(7), Table A1].

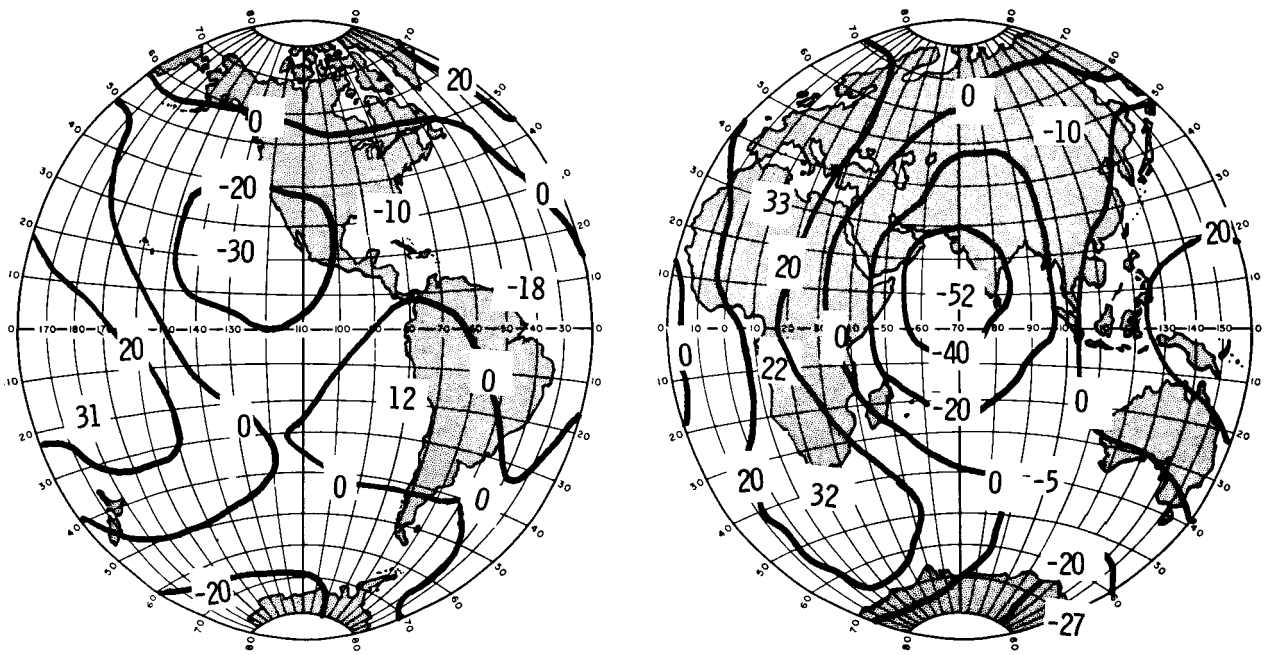

Figure A5—Satellite-camera geoid [(8), Table A1].

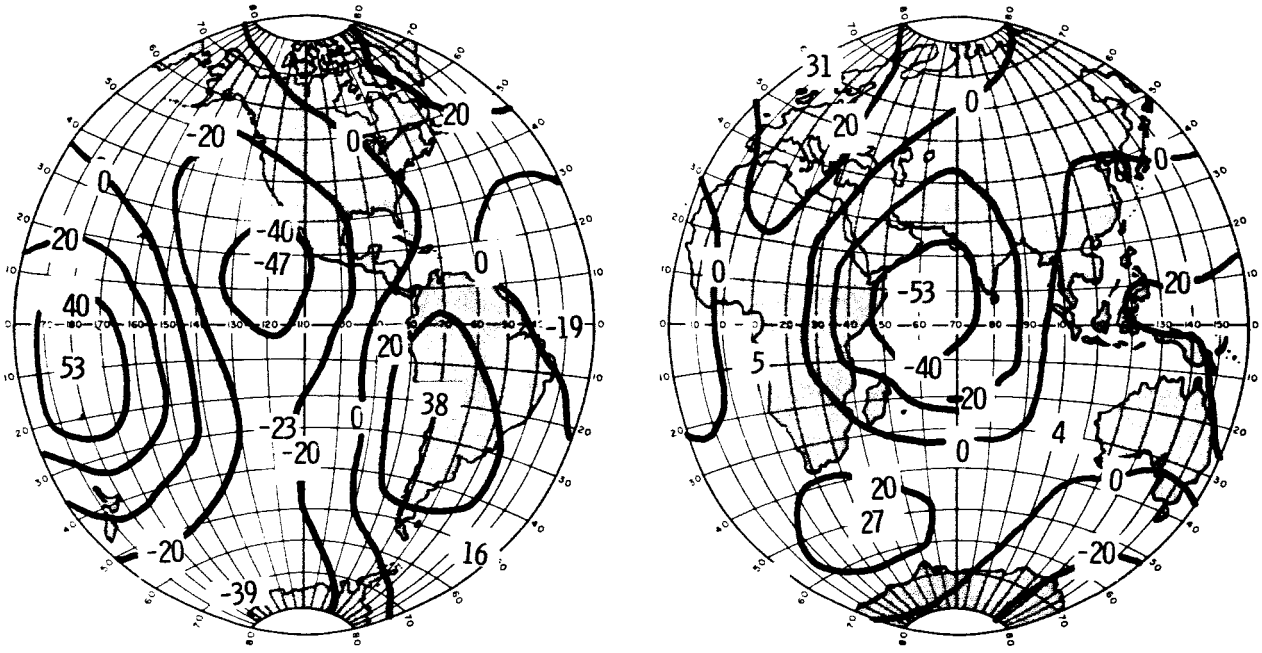

Figure A6—Satellite-camera geoid [(13), Table A1].

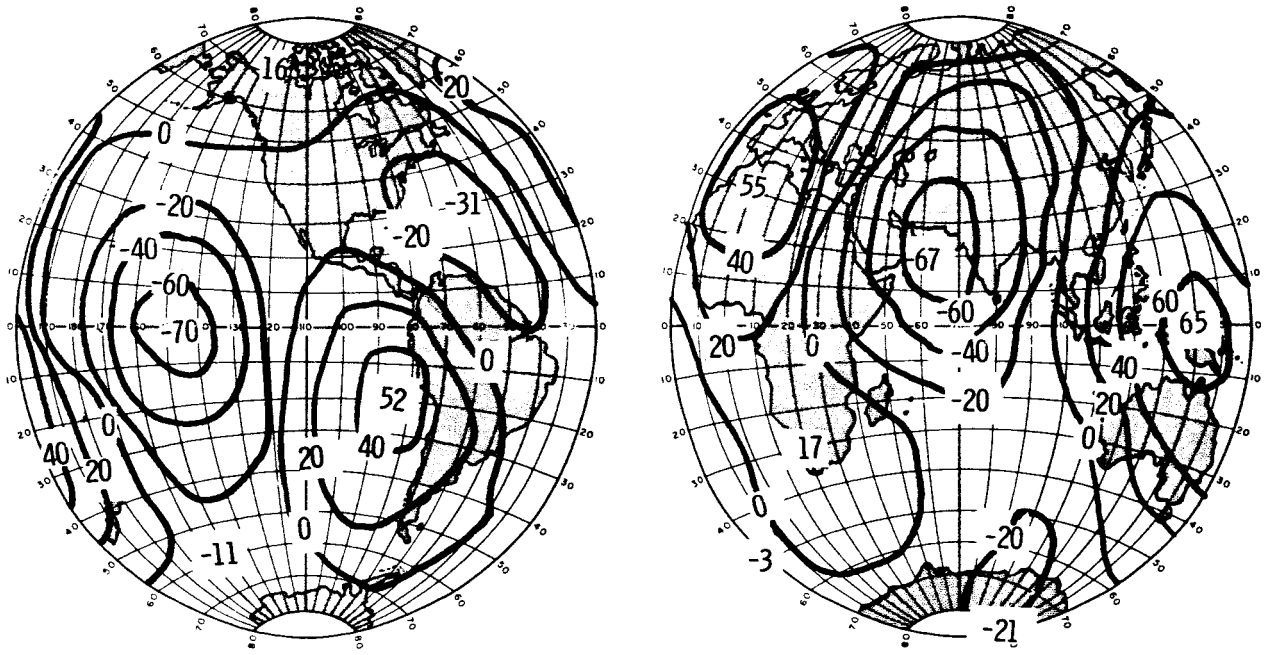

Figure A7—Surface-gravimetric geoid [(12), Table A1].

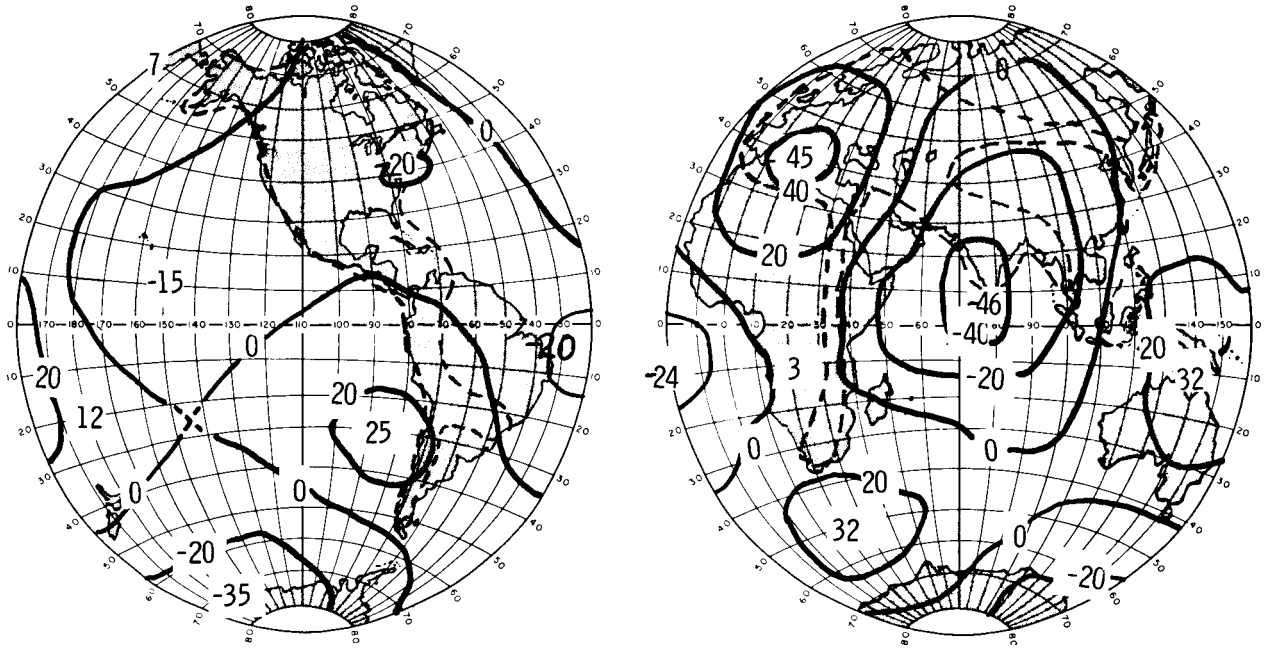

Figure A8—Combined astrogeodetic, gravimetric, and satellite geoid [(17), Table A1].

Appendix B

Expressions for the Inclination Factor

Equation 25 in the text gives the inclination factor in the drift causing tangential perturbation (due to equatorial ellipticity) on a 24-hour satellite with a near-circular orbit as

$$F(i) = \cos i + \frac{\Delta\lambda_{max} \sin^2 i}{2} \quad ; \tag{B1}$$

$\Delta\lambda_{max}$ is the absolute value of the maximum longitude excursion of the figure-8 ground track of the 24-hour satellite (with a near-circular orbit) from the geographic longitude of the nodes.

From Equation 18, this longitude excursion function is

$$\Delta\lambda = \lambda - \lambda_0 = \tan^{-1} \left(\cos i \tan\theta\right) - \theta \quad . \tag{B2}$$

Differentiating Equation B2 with respect to the argument angle θ, the minimax excursion arguments are found from

$$\frac{d(\Delta\lambda)}{d\theta} = 0 = \frac{\cos i \sec^2\theta}{1 + \cos^2 i \tan^2\theta} - 1 \quad . \tag{B3}$$

Solving Equation B3 for $\sin\theta$ at $\Delta\lambda_{minimax}$,

$$\sin\theta_{\Delta\lambda,minimax} = (\cos i + 1)^{-1/2} \quad ,$$

from which

$$\tan\theta_{\Delta\lambda,minimax} = (\sec i)^{1/2} \quad . \tag{B4}$$

Equation B4 in B2 gives

$$\Delta\lambda_{minimax} = \tan^{-1}(\cos i)^{1/2} - \tan^{-1}(\sec i)^{1/2} \quad .$$

Thus, since only the absolute value of $\Delta\lambda_{minimax}$ is required,

$$\Delta\lambda_{max} = \tan^{-1}(\sec i)^{1/2} - \tan^{-1}(\cos i)^{1/2} \quad , \tag{B5}$$

where the $\tan^{-1}$ is to be taken in the first quadrant. For example, for $i = 30$ degrees, Equation B5 evaluates the maximum excursion as

$$\Delta\lambda_{max} = 47.0\text{-}42.9 = 4.1 \text{ degrees} .$$

The nodal argument angle at this maximum longitude excursion is

$$\theta\left(\text{at } \Delta\lambda_{max}\right) = \pm 42.9 \text{ degrees from the nodes} .$$

The assumption in Equation 20 (in text) that the excursion in longitude from the ascending node could be approximated by

$$\Delta\lambda = -\Delta\lambda_{max} \sin 2\theta$$

predicts the maximum excursion argument as

$$\theta\left(\text{at } \Delta\lambda_{max}\right) = \pm 45 \text{ degrees from the nodes} .$$

This discrepancy in the assumed longitude excursion function is not serious until $i > 45$ degrees, as simulated trajectories with variable inclination have borne out.

Equation B5 can be written as

$$\Delta\lambda_{max} + \tan^{-1} (\cos i)^{1/2} = \tan^{-1} (\sec i)^{1/2} ,$$

from which

$$\tan\left(\Delta\lambda_{max} + \tan^{-1} (\cos i)^{1/2}\right) = (\sec i)^{1/2} = \frac{\Delta\lambda_{max} + (\cos i)^{1/2}}{1 - \Delta\lambda_{max} (\cos i)^{1/2}} , \tag{B6}$$

for $i < 45$ degrees. Solving Equation B6 for $\Delta\lambda_{max}$,

$$\Delta\lambda_{max} = \frac{1 - \cos i}{2(\cos i)^{1/2}} \doteq \frac{1 - \cos i}{1 + \cos i} , \tag{B7}$$

for i small.

Thus, the inclination factor becomes approximately

$$F(i) = \cos i + \frac{\sin^2 i\,(1 - \cos i)}{2(1 + \cos i)}$$

$$= \cos i + \frac{(1 - \cos i)^2}{2} = \frac{2\cos i + 1 - 2\cos i + \cos^2 i}{2}$$

$$= \frac{\cos^2 i + 1}{2} . \tag{B8}$$

For example, for $i = 30$ degrees,

$$F(i)_{\text{from Eq. B1}} = 0.86603 + 4.1/8 \times 57.3 = 0.8750 ,$$

$$F(i)_{\text{from Eq. B8}} = 0.8750 .$$

The agreement of $F(i)$ from forms B1 or B8 is good to the third decimal place as long as the inclination is less than 45 degrees. At inclinations higher than 45 degrees, however, the drift theory following Equation 20 (in text) begins to break down because $\Delta\lambda_{max}$ is no longer a small angle.

Appendix C

Reduction of Simulated Particle Trajectories for Earth-Equatorial Ellipticity

Tables C1 and C2 present data taken from two numerically integrated particle trajectories of a triaxial earth in the presence of the sun and moon's gravity field. Only perturbed equations of motion from a periodically rectified Keplerian reference orbit are actually integrated by the digital computer program (called ITEM at Goddard Space Flight Center). For the three months' real orbit time of these trajectories, the accumulated truncation and roundoff error in the numerical integration is believed to be negligible for the purposes of this reduction. The initial position and velocity conditions for these simulated trajectories were the same as those reported for the "actual" Syncom II orbits 1-2 (for the trajectory of Table C1) and 2-3 (for the trajectory of Table C2). The program used the earth gaussian-gravity constant

$$\mu_E = 3.9862677 \times 10^5 \text{ km}^3/\text{sec}^2 ,$$

which is the gravity constant used by the GSFC Data and Tracking Systems Directorate in computing the elements of satellite orbits from radar and Minitrack observations. The best estimates

Table C1

Data from Simulated Trajectory Beginning with the Elements of Syncom II Orbit 1-2

($J_{22} = -1.68 \times 10^{-6}$, $R_0 = 6378.388$ km, $\gamma_{22} = -108.0$: input into trajectory program)

Time from 26.709 Aug. 1963 (solar days)	Ascending Equator Crossing (degrees west of 50.0°W geog. long.)	Semimajor Axis (42160.0 + data; km)	Inclination (32.0 + data; degrees)
2.390	4.816	5.27	1.089
8.374	4.783	7.09	1.072
14.358	4.792	6.01	1.056
20.341	4.861	8.12	1.043
26.324	4.954	7.13	1.025
32.308	5.101	8.98	1.019
38.292	5.291	8.31	0.997
44.276	5.537	9.67	0.991
47.268	5.678	10.38	0.983
50.260	5.821	10.03	0.972
53.253	5.975	9.42	0.967
56.245	6.144	9.74	0.966
59.237	6.326	11.09	0.960
62.229	6.522	11.94	0.957

Table C2

Data from Simulated Trajectory Beginning with the Elements of Syncom II Orbit 2-3

($J_{22} = -1.68 \times 10^{-6}$, $R_0 = 6378.388$ km, $\gamma_{22} = -108.0$: input into trajectory program)

Time from 10.0 Dec. 1963 (days)	Ascending Equator Crossing (degrees west of 50.0°W geog. long.)	Semimajor Axis (42160.0 + data; km)	Inclination (32.0 + data; degrees)
0.823	9.243	6.88	0.881
5.809	9.351	7.30	0.881
10.796	9.495	9.41	0.877
15.783	9.666	8.15	0.864
20.769	9.885	9.85	0.864
25.756	10.134	10.60	0.850
30.743	10.401	9.95	0.842
35.730	10.708	11.81	0.841
40.717	11.044	12.18	0.825
45.704	11.412	11.58	0.816
50.692	11.830	13.93	0.808
55.679	12.259	13.11	0.790
58.672	12.534	13.07	0.785
60.667	12.724	13.69	0.784

(in the "least squares" sense) of the coefficients $(d)_{s1}$ and $(e)_{s1}$, obtained by fitting the drift and orbit expansion text equations 66 and 67 to the data in Table C1, have been found to be

$$(d_0)_{s1} \approx 4.841 \pm 0.004 \text{ degrees},$$

$$(d_1)_{s1} \approx -(1.22 \pm 0.03) \times 10^{-2} \text{ degree/solar day},$$

$$(d_2)_{s1} \approx (6.303 \pm 0.038) \times 10^{-4} \text{ degree/solar day}^2,$$

$$= (6.268 \pm 0.038) \times 10^{-4} \text{ degree/sid. day}^2,$$

$$(e_0)_{s1} \approx 5.45 \pm 41 \text{ km},$$

$$(e_1)_{s1} = 0.091 \pm 0.010 \text{ km/solar day},$$

$$\approx 0.091 \pm 0.010 \text{ km/sid. day}.$$

The mean value of the inclination during this first simulated trajectory period was

$$i_{s1} = 33.005 \pm 0.003 \text{ degrees}.$$

From Equation 69,

$$(T_0)_{s1} = 9.68 \pm 0.30 \text{ days from } 26.709 \text{ August } 1963 .$$

From Equation 70, in the text,

$$(\lambda_0)_{s1} = \left(4.782 \begin{smallmatrix} +.008 \\ -.007 \end{smallmatrix}\right) \text{degrees west of } 50°\text{W long} .$$

From Equation 71,

$$(\ddot{\gamma}_0)_{s1} = -(1.261 \pm 0.008) \times 10^{-3} \text{ degree/solar day}^2$$

$$= -(2.188 \pm 0.013) \times 10^{-5} \text{ rad/sid. day}^2 .$$

From Equation 73, and the above value of $(T_0)_{s1}$,

$$(a_s)_{s1} = 42166.3 \pm 0.4 \text{ km} .$$

The best estimates (in the "least squares" sense) of the coefficients $(d)_{s2}$ and $(e)_{s2}$, obtained by fitting the drift and orbit expansion Equations 66 and 67 to the data in Table A2, have been found to be

$$(d_0)_{s2} = 9.224 \pm 0.004 \text{ degrees}$$

$$(d_1)_{s2} = (1.830 \pm 0.028) \times 10^{-2} \text{ degree/solar day}$$

$$(d_2)_{s2} = (6.501 \pm 0.042) \times 10^{-4} \text{ degree/solar day}^2$$

$$= (6.465 \pm 0.042) \times 10^{-4} \text{ degree/sid. day}^2$$

$$(e_0)_{s2} = 7.19 \pm 0.37 \text{ km}$$

$$(e_1)_{s2} = 0.111 \pm 0.010 \text{ km/solar day}$$

$$= 0.111 \pm 0.010 \text{ km/sid. day} .$$

The mean value of the inclination during the second simulated trajectory period is

$$i_{s2} = 32.836 \pm 0.003 \text{ degrees} .$$

From Equation 69,

$$(T_0)_{s2} = -(14.07 \pm 0.30) \text{ days from 10.0 December 1963 .}$$

From Equation 70,

$$(\lambda_0)_{s2} = \left(9.095 \begin{smallmatrix} +.009 \\ -.009 \end{smallmatrix}\right) \text{degrees west of 50.0°W long .}$$

From Equation 71,

$$(\ddot{\gamma}_0)_{s2} = -(1.300 \pm 0.008) \times 10^{-3} \text{ degrees/solar day}^2$$

$$= -(2.257 \pm 0.015) \times 10^{-5} \text{ rad/sid. day}^2 \quad .$$

From Equation 73, and the above value of $(T_0)_{s2}$,

$$(a_s)_{s2} = 42165.6 \pm 0.5 \text{ km .}$$

A graph of these trajectory simulations is seen in Figure C1.

Combining the above results for the two simulated trajectories, from Equation 60,

$$\frac{(A_{22})_{s1}}{(A_{22})_{s2}} = (42165.6 \pm 0.5/42166.3 \pm 0.4)^2 \left[\frac{\cos^2(33.005 \pm 0.003) + 1}{\cos^2(32.836 \pm 0.003) + 1}\right]$$

$$= 0.99840 \pm 0.00007$$

$$\nabla\lambda = (\lambda_0)_{s2} - (\lambda_0)_{s1} = -(59.095 \pm 0.009) - [-(54.782 \pm 0.008)] ,$$

$$\therefore 2\nabla\lambda = -(8.626 \pm 0.034) \text{ degrees geographic long .}$$

Therefore, from Equation 58, the location of the minor equatorial axis with respect to the "synchronous longitude" during the first simulated trajectory (54.782 ± 0.008 degrees west of Greenwich) is

$$(\gamma_0)_{s1} = \frac{1}{2} \tan^{-1} \left\{ \frac{\sin[-(8.626 \pm 0.034)]}{\frac{1.300 \pm 0.008}{1.261 \pm 0.008}(0.99840 \pm 0.00007) - \cos[-(8.626 \pm 0.034)]} \right\}$$

$$= 52.5 \pm 2.5 \text{ degrees east of the minor equatorial axis .}$$

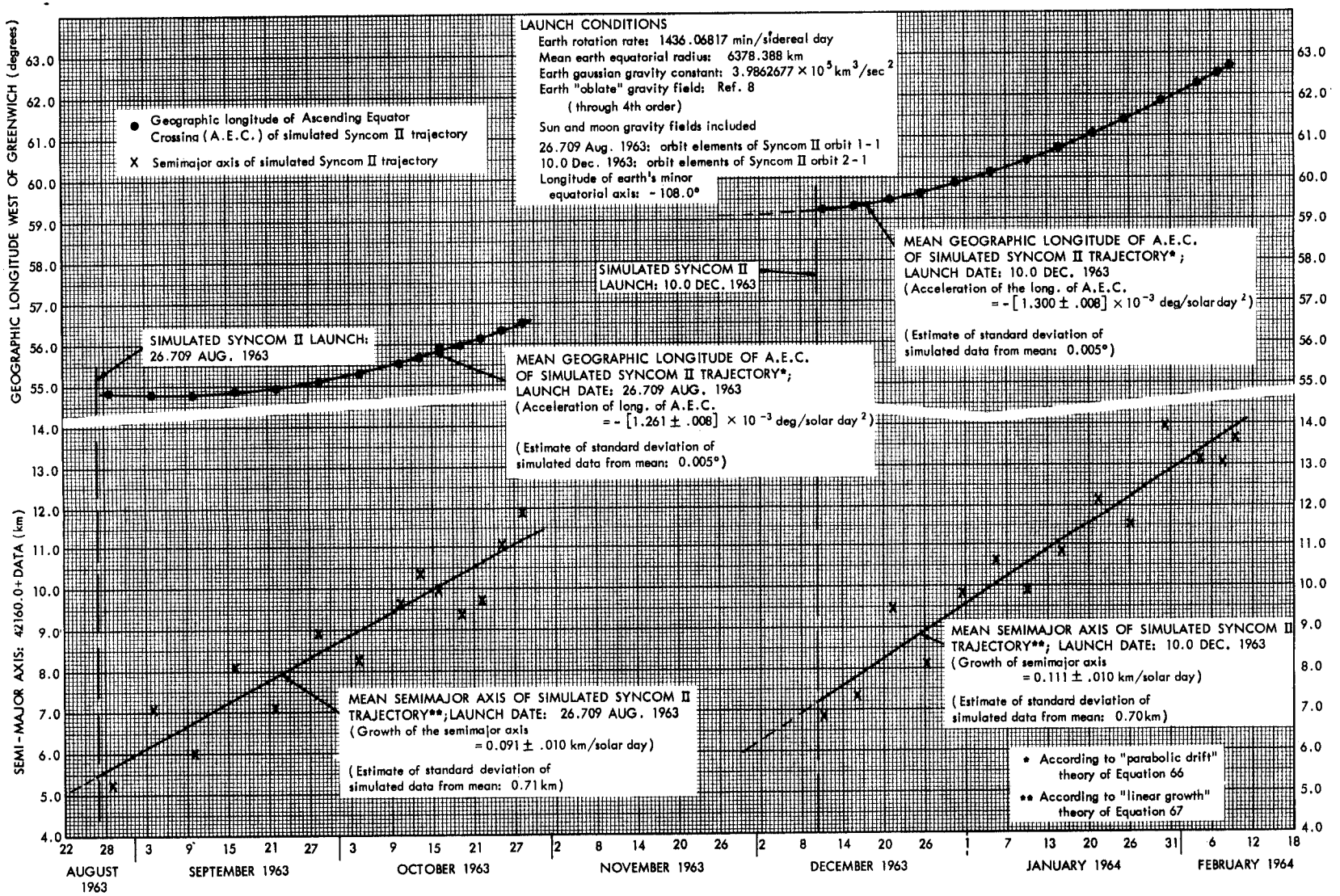

Figure C1—Drift of the ascending equator crossing and growth of the semimajor axis of simulated Syncom II trajectories.

From Equation 60a, the best estimate of the geographic location of the nearest extension of the equatorial minor axis from the simulated trajectory data is

$$(\gamma_{22})_s = -54.8 - (52.5 \pm 2.5) = -(107.3 \pm 2.5) \text{ degrees geographic long .}$$

This compares well with the input value of $(\gamma_{22})_s = -108.0$ degrees used to compute the simulated trajectories. From Equation 59, the best estimate of the triaxial gravity coefficient J_{22} from the simulated data (according to the theory of this report) is

$$(J_{22})_s = \frac{-(2.188 \pm 0.013) \times 10^{-5}}{72\pi^2 \left[\sin 2(52.5 \pm 2.5)\right] (6378.388/42166.3 \pm 0.4)^2 \left[\frac{\cos^2 (33.005 \pm 0.003) + 1}{2}\right]}$$

$$= -(1.64 \pm 0.03) \times 10^{-6} .$$

The mean equatorial radius used in the simulation is $R_0 = 6378.388$ km, the same used to compute the "actual" Syncom II orbits from the radar and Minitrack observations.

The above value of $(J_{22})_s$ compares reasonably well with the input value of $(J_{22})_s = -1.68 \times 10^{-6}$ used to compute the simulated trajectories.

The model error implicit in the difference between the reduced and inputed geodetic coefficients for the simulated trajectories warrants an adjustment of the J_{22} and λ_{22} reported in the section on the reduction of the "actual" Syncom II orbits. The values below appear sufficient to cover all the uncertainties of this reduction for a triaxial earth:

$$J_{22} \text{ (reduced for a triaxial earth)} = -(1.70 \pm 0.05) \times 10^{-6} ,$$

$$\lambda_{22} \text{ (reduced for a triaxial earth)} = -(19 \pm 6) \text{ degrees geographic long .}$$

As the introduction indicates, the principal effect unaccounted for in the reduction is the possible influence of higher order earth tesseral anomalies on the drift of Syncom II. Figure A1 indicates that the accumulated influence on synchronous satellites of all higher order anomalies is small compared with the second-order anomaly according to recent satellite geoids. Close and continuing observations on the drift of 24-hour satellites will clarify this assumption, and should be rewarded in time by revelation of the "tesseral" anomalies through third-order with an absolute precision almost as good as that reported here for the second-order effect.

Appendix D

Basic Orbit Data Used in this Report

The Orbit elements for Syncom II in Table D1 were calculated at the GSFC Tracking and Data Systems Directorate from radar and Minitrack observations made during the slow-drift periods from mid-August 1963 to February 1964.

As an example of the estimation of the ascending equator crossing nearest to epoch, consider the orbit geometry at epoch (Figure D1): 6 January 1964 at 17.0 hours Universal Time (orbit 2-5).

Table D1

Syncom II Orbital Elements, August 1963 to February 1964

Orbit	Epoch (Universal Time) (year-month-day-hour-min-sec)	Semimajor Axis (km)	Eccentricity	Inclination (degrees)	Mean Anomaly (degrees)	Argument of Perigee (degrees)	Right Ascension of the Ascending Node (degrees)
1-1	63-8-22-6-12-8	42164.58	0.00018	33.083	24.126	26.285	317.569
1-2	63-8-26-17-0	42164.52	0.00016	33.090	190.841	26.099	317.454
1-3	63-8-31-0-0	42166.02	0.00018	33.062	296.125	30.073	317.475
1-4	63-9-5-0-0	42166.39	0.00012	33.064	333.521	357.756	317.362
1-5	63-9-9-0-0	42166.35	0.00015	33.048	326.207	9.077	317.272
1-6	63-9-12-2-0	42166.55	0.00015	33.079	3.657	4.697	317.224
1-7	63-9-17-2-0	42166.70	0.00018	33.043	12.694	0.581	317.165
1-8	63-9-20-2-0	42167.42	0.00018	33.010	359.970	16.282	317.098
1-9	63-9-27-2-0	42167.51	0.00022	33.046	38.922	344.162	316.996
1-10	63-10-1-2-0	42168.88	0.00024	33.039	26.615	0.433	316.944
1-11	63-10-8-2-0	42169.14	0.00020	33.013	42.889	350.866	316.780
1-12	63-10-14-2-0	42169.78	0.00028	32.982	36.727	2.673	316.813
1-13	63-10-22-2-0	42171.51	0.00026	32.993	62.833	344.246	316.603
1-14	63-10-30-0-0	42171.09	0.00028	32.948	29.865	354.548	316.570
1-15	63-11-6-0-0	42172.15	0.00025	32.952	36.699	354.313	316.328
1-16	63-11-12-5-0	42172.51	0.00031	32.920	108.239	3.425	316.308
2-1	63-11-28-1-0	42165.89	0.00005	32.920	222.170	203.901	315.976
2-2	63-12-4-0-0	42167.20	0.00009	32.892	39.435	17.564	315.919
2-3	63-12-10-0-0	42167.18	0.00010	32.881	51.942	10.958	315.877
2-4	63-12-16-17-0	42168.17	0.00007	32.872	300.000	24.505	315.735
2-5	64-1-6-17-0	42168.01	0.00013	32.867	332.997	11.625	315.544
2-6	64-1-9-6-0	42169.90	0.00015	32.857	165.031	16.992	315.469
2-7	64-1-20-21-0	42171.43	0.00012	32.826	29.098	28.842	315.300
2-8	64-1-29-20-0	42171.91	0.00019	32.859	37.956	13.171	315.212
2-9	64-2-5-16-0	42172.89	0.00019	32.800	321.168	36.275	315.075
2-10	64-2-10-19-0	42173.31	0.00014	32.833	32.517	14.553	314.982
2-11	64-2-17-17-0	42174.89	0.00019	32.762	347.774	35.551	314.883

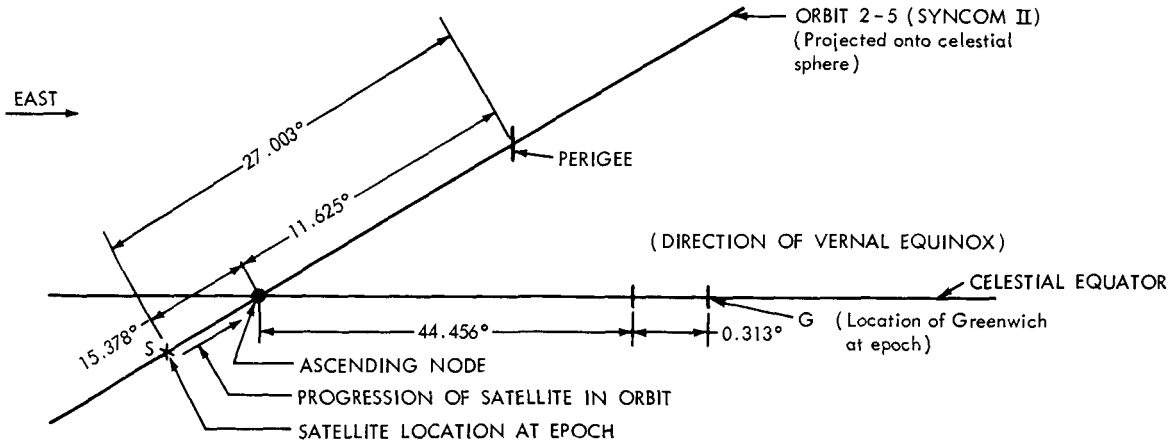

Figure D1—A portion of the celestial sphere at the epoch of orbit 2-5.

On 6.0 January 1964, the hour angle of the vernal equinox *west* of Greenwich (expressed in hours, with 24 hours = 360 degrees) was

6 hr 58 min 27.484 sec (from the Nautical Almanac) .

On 7.0 January 1964, the hour angle of Ω was

7 hr 2 min 24.036 sec .

Interpolating, the hour angle of Ω on 6 January at 17 hours Universal Time was

0 hr 1 min 15.042 sec, or

0.313 degrees west of Greenwich .

In Figure D1, the orbit angle 27.003 degrees is taken directly as 360 degrees minus the mean anomaly, because the orbit is nearly circular. The reported period for this orbit was

$$T_p = 1436.21696 \text{ min} .$$

The earth's sidereal rotation period is taken to be

$$T_{earth} = 1436.06817 \text{ min} .$$

Thus, if the satellite is assumed to traverse orbit 2-5 at a nearly uniform rate, it will reach the celestial equator at a time when the Greenwich meridian has proceeded eastward from the epoch

$$15.378 \times 1436.21696/1436.06817 = 15.380 \text{ degrees} .$$

Thus, the estimated geographic longitude of the ascending equator crossing nearest to the epoch of orbit 2-5 is

$$\text{Ascending equator crossing longitude} = -(44.456 + 0.313 + 15.380)$$

$$= -60.149 \text{ degrees (see Table 1).}$$

The estimated time of this crossing is

$$\frac{15.380^\circ}{15^\circ/\text{hr}} = 1.025 \text{ hours after the epoch .}$$

The crossing time (Table 1 in text) is thus estimated to be at

6.751 January 1964 (18.025/24 + 6.0 January 1964) .

Appendix E

Derivation of Exact Elliptic Integral of Drift Motion for a 24-Hour Near-Circular Orbit Satellite: Comparison of Exact Solution with Approximate Solutions for Periods Very Close to Synchronous

The differential text equation 33 of 24-hour satellite drift is analogous to the equation describing the large-angle oscillations of a mathematical pendulum (see Reference 10), as in Figure E-1.

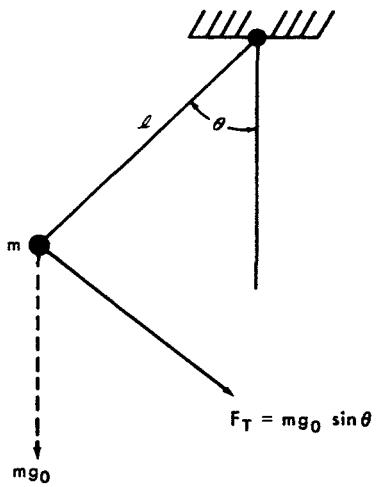

Figure E1—Configuration of a "mathematical pendulum."

The equation of angular motion of the mass m under the constant gravity force mg_0 is

$$F_T = mg_0 \sin\theta = \frac{md^2(l\theta)}{dt^2} = ml\ddot{\theta} . \qquad \text{(E1)}$$

Equation E1 can be rewritten as

$$\ddot{\theta} + (g_0/l) \sin\theta = 0 . \qquad \text{(E2)}$$

From the theory developed in Reference 10 (pp. 327-335), Equation E2 has an integral

$$t(\text{time from } \theta = 0) = (l/g_0)^{1/2} F(\underline{k}, \phi) , \qquad \text{(E3)}$$

where $F(\underline{k}, \phi)$ is the elliptic integral of the first kind with argument (or amplitude)

$$\phi = \sin^{-1}\left(\frac{\sin\theta/2}{\sin\theta_{max}/2}\right)$$

and modulus

$$\underline{k} = \sin\theta_{max}/2.$$

Equation 33 in the text,

$$\ddot{\gamma} + A_{22} \sin 2\gamma = 0 ,$$

with maximum libration angle γ_0, can be put in the form of Equation E2 by the transformation of the dependent variable

$$\theta = 2\gamma \tag{E4}$$

with the parameter identification

$$g_0/l = 2A_{22} . \tag{E4a}$$

Equation E4 implies the identification

$$\underline{k} = \sin\gamma_0 , \qquad \underline{\phi} = \sin^{-1}\left(\sin\gamma/\sin\gamma_0\right) . \tag{E4b}$$

The pendulum solution (Equation E3), under the transformation E4 and identifications E4a and E4b, becomes

$$t\,(\text{time of drift libration from } \gamma = 0) = \left(1/2A_{22}\right)^{1/2} F\left[\sin\gamma_0,\ \left(\sin^{-1}\sin\gamma/\sin\gamma_0\right)\right] . \tag{E5}$$

$F(\underline{k}, \underline{\phi})$, in its full integral form, is

$$F = \int_0^{\underline{\phi}} \frac{d\underline{\phi}}{\left(1 - \underline{k}^2 \sin^2\underline{\phi}\right)^{1/2}} , \tag{E6}$$

(where $\underline{k}^2 = \sin^2\gamma_0$, $\sin^2\underline{\phi} = \sin^2\gamma/\sin^2\gamma_0$) for the drift libration. In particular, when $\underline{\phi} = \pi/2$, then $\gamma = \gamma_0$; $\dot{\gamma}_0 = 0$; and the pendulum-drift libration has completed a quarter-period.

Thus, from Equations E5 and E6, the full period of the long-term drift libration of the 24-hour satellite ground track about the nearest minor equatorial axis longitude is

$$T(\gamma_0) = \left(8/A_{22}\right)^{1/2} \int_0^{\pi/2} \frac{d\psi}{\left(1 - \sin^2\gamma_0 \sin^2\psi\right)^{1/2}} . \tag{E7}$$

The adequacy of the Taylor series expansion approximation of the drift motion in the neighborhood of γ_0, given in Equation 50, may be tested against the exact drift solution implicit in Equation E5. Table E1 gives the evaluation of F for arguments within 5 degrees of $\gamma_0 = 60$ degrees, using the integral tables in Reference 11. In Table E1, ΔF is the change in the elliptic integral from the "stationary" configuration at $\gamma = 60$ degrees or $\underline{\phi} = 90$ degrees; $\Delta t = \left(1/2A_{22}\right)^{1/2} \Delta F$; A_{22} was computed from Equation 30a with the following gravity-earth constants and for the inclination of Syncom II:

$$R_0 = 6378.2 \text{ km} ,$$

$$a_s = 42166 \text{ km} ,$$

$$J_{22} = -1.7 \times 10^{-6},$$

$$i = 33 \text{ degrees}.$$

γ' gives the drift position as calculated from the first right-hand term of Equation 50 alone [the $(\Delta t)^2$ term]. γ'' gives the drift position as calculated from the first two right-hand terms of 50. The "actual" Syncom II drift in mid-August 1963 began, apparently, at a γ_0 between 48 and 58 degrees east of the minor axis. Thus, the 16 orbits chosen for the first drift period all should be well represented by the $(\Delta t)^2$-only theory, within the rms error of the longitude observations. Similar exact calculations for γ_0 = 45, 50, and 55 degrees confirm the adequacy of the $(\Delta t)^2$-only theory to apply to the second drift-period orbits. They also prove the contention in the section on approximations to exact drift solutions (p. 16 ff.) that, for reasonably small excursions from "synchronism", the convergence of the Taylor series (Equation 50) is adequate if additional terms are included only when they become of a certain minimum significance to the total drift.

Table E1

Exact and Approximate Drifts of a 24-Hour Satellite from a Stationary Configuration 60° East of the Earth's Minor Equatorial Axis

γ_0 = 60 degrees	γ (degrees)	γ' (degrees)	γ'' (degrees)	Φ (degrees)	F (rad)	ΔF (rad)	Δt (days from) γ = 60°
$A_{22} = 23.2 \times 10^{-6}$ rad/day^2	60.0	60.0	60	90	2.1565	-	-
	59.0	59.003	59.000	81.7967	1.8730	0.2835	41.619
	58.0	58.014	58.001	78.3056	1.7564	0.4001	58.737
	57.0	57.029	56.999	75.5595	1.6671	0.4894	71.846
	56.0	56.051	56.999	73.1938	1.5923	0.5642	82.827
	55.0	55.077	54.996	71.0617	1.5265	0.6300	92.487

Appendix F

List of Symbols

A_{22} Driving function causing drift and orbit expansion of a 24-hour satellite in a "triaxial" earth-gravity field; a constant for a given 24-hour orbit inclination

a, a_s Instantaneous semimajor axis, and "momentarily synchronous" semimajor axis, of orbit of the 24-hour earth satellite. (a_s, estimated to within 3 km, is 42166 km)

a_0, b_0 Major and minor equatorial radii of the "triaxial" earth [$R_0 = (a_0 + b_0)/2$, according to definition in Wagner, *op. cit.;* see footnote, p. 7]

a_1 $(a - a_s)/a_s$; a nondimensional semimajor axis change for the 24-hour satellite's orbit, with respect to "momentarily synchronous" semimajor axis

ds A small arc length of a space trajectory

(d_n), (e_n) Determinable coefficients in drift and orbit-expansion equations 67 and 68

F A gravity force per unit mass acting on a 24-hour satellite

$F(i)$ Inclination factor in the triaxial driving function A_{22}

$F(\underline{k}, \phi)$ Elliptic integral of the first kind with argument (or amplitude) ϕ and modulus $\underline{k}$

g_0, g_s Radial acceleration of the earth's gravity field at the earth's surface and at altitude of the "synchronous" satellite

i Inclination of orbit of the 24-hour satellite

J_{nm}, λ_{nm} Spherical harmonic constants (order n, power m)* of the earth's gravity potential

M Mean anomaly of the satellite in its orbit: orbit angle (from center of the earth) from perigee to a point M in the orbit, where $M = 2\pi t/T_p$, t being real time since perigee passage and T_p period of the satellite's orbit

m A test mass

R_0 Mean equatorial radius of the earth (6378.2 km)

*In the literature of *spherical* harmonics n is often called "degree," and m "order." However, in speaking of the *order* of influence of the *gravitational* harmonics, n is generally used. For this reason, the author prefers the nomenclature "order" for n and "power" or "degree" for m when referring to gravitational harmonics.

T_p, T_s Orbital period for a satellite, and "momentarily synchronous" period of a 24-hour satellite (i.e., the earth's sidereal rotation period)

T_0 Time of "synchronism" from an arbitrary base time of reckoning T

t Real time

V_E Gravity potential of the earth

w Argument of perigee in a satellite orbit: orbit angle (from center of the earth) from ascending node to perigee

$( )_0$ Argument ( ) at start of dynamics under consideration

$( )_n$ Argument ( ) at a specified location n [except in Appendix C: ( )s; argument for the simulated trajectory]

$\dot{( )}, \ddot{( )}, ( )^{[n]}$ $\frac{d( )}{dt}, \frac{d^2( )}{dt^2}, \frac{d^n( )}{dt^n}$: time differentials

$\Delta( )$ A small argument ( )

γ Geographic longitude (positive to the east) of the 24-hour satellite, or ascending equator crossing of the satellite's orbit with respect to longitude of the earth's minor equatorial axis

γ_0 Geographic longitude (positive to the east) of ascending equator crossing of the 24-hour satellite's orbit with respect to the earth's minor equatorial axis' longitude location, at start of dynamics under consideration

θ Argument from ascending node to satellite position for the 24-hour orbit

λ, r, ϕ Geographic longitude, geocentric radius, and geocentric latitude of the 24-hour satellite position

λ_0 "Initial" geographic longitude of the satellite, or ascending node of the 24-hour satellite's orbit at start of dynamics under consideration

$\nabla\lambda$ Geographic longitude difference between two "momentarily synchronous" 24-hour satellite configurations

μ_E Earth's gaussian gravity constant (3.986×10^5 km^3/sec^2)

Ω Longitude location of the vernal equinox

ω_e Earth's sidereal rotation rate (0.7292115×10^{-4} rad/sec)